ELECTROPHORETIC DEPOSITION OF METALLIC OXIDES TiO_2, NiO, Cr_2O_3 AND Al_2O_3 FROM AQUEOUS SUSPENSIONS

By

JAYANT YASHAVANT CHOUDHARY

DEPARTMENT OF METALLURGICAL ENGINEERING

INDIAN INSTITUTE OF TECHNOLOGY, KANPUR

June, 1978

ELECTROPHORETIC DEPOSITION OF METALLIC OXIDES TiO_2, NiO, Cr_2O_3 AND Al_2O_3 FROM AQUEOUS SUSPENSIONS

A Thesis Submitted
In Partial Fulfilment of the Requirements
for the Degree of
MASTER OF TECHNOLOGY

By
JAYANT YASHAVANT CHOUDHARY

to the
DEPARTMENT OF METALLURGICAL ENGINEERING
INDIAN INSTITUTE OF TECHNOLOGY, KANPUR
June, 1978

Electrophoretic coatings from Organic Solutions

Fahnoe and co-workers[28] deposited aluminium oxide and nickel oxide particles of very fine size (325 mesh) from thick paste in isopropyl alcohol, with a direct current under 100 V applied for 10 seconds. The suspension produced a cathodic coating approximately 0.4×10^{-4} inch thick, with an electrode spacing of 3 cm. After appropriate post treatments, the coating was useful as metal bonded abrasive surfaces for precision laps and dies.

Benjamin and Osborn [6] investigated the deposition of carbonates of barium-strontium (0.5 - 50 μ particle diameter) using nitrocellulose binder and acetone as the suspension media. To reduce particle settling and solvent evaporation, small quantities of ethylene glycol were added.

Senderof and Reid [26] have deposited dense barium titanate on metal sheets. The appropriate amounts of $BaTiO_3$, diethyl glycol, dimethyl ether, and kentol-60 were mixed and ball milled for about 18 hours. The additional amounts of dimethyl compounds were added and milling continued for another 2 hours. The resultant colloidal suspension was used for electrophoretic deposition with a metal screen cathode and a metal sheet anode. Deposits approximately 0.003 inch. thick were obtained on the anode in about one

ACKNOWLEDGEMENTS

I take this opportunity to express my gratitude to Dr. H.S. Ray and Dr. K.N. Rai for their valuable guidance and constant encouragement at all the stages of this work.

I wish to offer my thanks to Indian Space Research Organization, Department of Space (Govt. of India) for sponsoring this project with financial support.

I am very thankful to Drs. A. Ghosh and G.S. Upadhyaya for various discussions and voluable suggestions throughout this investigative work. I am indeed grateful to Dr. A. Ghosh for providing me with various materials and instrumental facilities. My thanks are also due to Dr. K.S. Gandhi, Dr. U.M. Bokare (Chemical Engg.) and Dr. Malay Choudhary (Environmental Engg.) for providing me the facilities to use viscometer and zetameter respectively.

I am particularly indebted to my friend N.B. Ballal for his selfless help and co-operation. His assistance has been a source of inspiration at all the crucial stages of this work.

I really admire Mr. A. Sharma for his excellent co-operation and his valuable help without whose

help the whole efforts would have been defeating.

My thanks also goes to Dr. Kar (Electrical Engg.) for providing me with deionized water throughout the course of this work.

I am grateful to my friends Messers B.H. Narayana, R.K. Dixit, S.R. Prabhakar, H. Dharwadkar, A.S. Moharir, B.C. Patwardhan and many others for their help in various ways.

Finally, I wish to express my thanks to Mr. V.P. Gupta for sketching the figures and Ms. C. Komala for neat typing the manuscript.

(JAYANT CHOUDHARY)

CONTENTS

PREFACE

Electrophoresis has been successfully employed in painting technology, medicine and biological separation work. Here an attempt has been made to apply this technique in coating of metallic oxides on conducting substrates from water media. The historical developments and principles of electrophoretic deposition are discussed in the first two chapters. The results of detailed investigation on phenomenon of electrophoretic transport and optimum coating conditions are presented in the third chapter. The fourth chapter deals with an afford made to develope oxidation resistant alumina coatings on graphite rods and preparation of Ni-Cr-Fe composite on mild steel plates.

LIST OF FIGURES

LIST OF TABLES

CHAPTER 1

INTRODUCTION

Though electrophoresis is known from a long time, recently it has drawn the attention of quite a few research workers because of its technological importance. This chapter is therefore exclusively devoted to outlining the historical development with special imphasis on metallurgical application and relevant literature review.

1.1 Electrophoresis

Electrophoresis is the phenomenon associated with the movement of colloidal particles, suspended in an aqueous or non-aqueous media in an electrical field.

1.2 History

The phenomenon of electrophoresis was discovered in 1808 by Reuss[13], a Russian physicst, who found that when electricity was passed through a glass tube containing a water suspension of clay, the clay particles migrated towards the positive electrode. Electrophoresis is believed to have been first used for metal and metal oxide deposition in 1927 by Harsani[28], who applied the process to deposit tungston and thorium oxides on platinum cathodes. Since then wide spread applications have been made in the electronics, wire,

rubber, ceramics and other industries[7]. The study of deposition from aqueous systems was not tackled academically until 1948, and not until 1963 was the first full scale industrial plant in operation [5].

1.3 Applications

Although the phenomenon of electrophoresis has been observed and investigated for almost 100 years, only limited use has been made of electrophoresis as a method of applying coatings to materials. Early investigators[3] concerned themselves with depositing coatings such as rubber latex, but these were not required to adhere the substrate, which was essentially a mold. A technique for coating the inside of tin cans with wax was also developed[1] but never applied.

The interesting metallurgical applications of electrophoresis have been revived in recent years [10-12,15,18,22] The process of electrophoresis may give rise to several possibilities.

(1) The refractory oxide coatings on metal substrates can be obtained after sintering.

(2) The oxide coating can be carburized to give hard wear resistant carbide coats on metal substrate.

(3) The metallic coatings can be easily obtained after reduction of oxide coatings. In case of two oxides co-deposited, alloys may be formed.

(4) It is possible to produce metal-oxide composite coat through preferential reduction of one oxide in a oxide mixture.

(5) The method has also been applied in fabrication of ceramic tubes and crucibles.

(6) The deposit may also be transformed into porous membranes for various end uses, e.g. electrolytic cells, filters etc.

1.4 Literature Review

Although the phenomenon of electrophoretic deposition was discovered a century ago its exploitation in laboratory investigation or commercial application has been slow and sporadic. For example although a technique for coating the inside surface of tin cans by wax was described in the literature[1], the technique was neither persuaded in the laboratory nor applied commerically. Moreover, most of the early investigations were non-metallurgical in nature. Some of the poineering investigations, which are of direct relevance to metallurgists, are briefly reviewed below.

Electrophoretic coatings from Organic Solutions

Fahnoe and co-workers[28] deposited aluminium oxide and nickel oxide particles of very fine size (325 mesh) from thick paste in isopropyl alcohol, with a direct current under 100 V applied for 10 seconds. The suspension produced a cathodic coating approximately 0.4×10^{-4} inch thick, with an electrode spacing of 3 cm. After appropriate post treatments, the coating was useful as metal bonded abrasive surfaces for precision laps and dies.

Benjamin and Osborn [6] investigated the deposition of carbonates of barium-strontium (0.5 - 50 μ particle diameter) using nitrocellulose binder and acetone as the suspension media. To reduce particle settling and solvent evaporation, small quantities of ethylene glycol were added.

Senderof and Reid [26] have deposited dense barium titanate on metal sheets. The appropriate amounts of $BaTiO_3$, diethyl glycol, dimethyl ether, and kentol-60 were mixed and ball milled for about 18 hours. The additional amounts of dimethyl compounds were added and milling continued for another 2 hours. The resultant colloidal suspension was used for electrophoretic deposition with a metal screen cathode and a metal sheet anode. Deposits approximately 0.003 inch. thick were obtained on the anode in about one

minute using voltages between 500 to 2000 V.

Werner and Ride Jr. [31] deposited alloy containing 80 percent Nickel and 20 percent Chromium using a suspension of metal and metal oxide powder in isopropyl alcohol, nitromethane, and zein solution. Coatings 2 to 3 x 10^{-4} inch thick were obtained on the cathode in 30 to 60 seconds at 20 V. After the deposition the coatings were densified and sintered to produce a dense structure with oxidation resistant properties.

Coatings of a number of elements (B, Zr, Nb, Au, Mo, W and others) have been attempted using a similar technique by Guthierrez, Mosley and Wallace [18] The particle size ranged from 1 μ to 20 μ, the optimum size being about 6 μ. It was found that deposition rate increased with voltage at low voltages (upto 700 Volts) and decreased with voltage at high voltages (upto 2500 Volts). However, the suspending media used were isopropyl alcohol and nitromethane, thereby accounting for high voltages necessary for deposition.

Using electrophoretic techniques, ceramic wares were prepared by Andrews et.al. [4] Powers [23] and many others. Powers used those alcohols as vehicles which had dielectric constants in the range of 12 to 24 and specific conductance in the range of 10^{-7} to 10^{-4} mho cm^{-1}. He deposited β alumina

on stainless steel electrodes and after deposition, alumina tubes came off easily from the mandrel, which had very high surface finish.

Electrophoretic Coatings from Aqueous Solutions

Only limited number of studies on deposition from aqueous solutions have been reported in the literature. Some of the recent investigations are as follows.

A study of Fisch [15] on the electrophoretic deposition of aluminide coatings from aqueous suspensions used an amine-solubilized acrylic resin as a dispersant in distilled water. The pH of the bath was 7.8 to 8.3, and the aluminium flake particle size was 7.5 μ or less. The voltages used in the deposition was between 25 volts and 70 volts.

Kucharski [22] has reported successful electrophoretic deposition of thick WO_3 and Cr_2O_3 coatings from an aqueous suspension containing 22 g of oxide per 100 ml of water. These coatings were carburized at higher temperatures, using $CO-CO_2$ mixture to produce hard and wear resistant carbide surfaces.

Caley[10] have investigated electrophoretic transport for the suspension of oxides NiO, Cr_2O_3, Fe_2O_3, MnO and TiO_2 in aqueous suspension. Electrophoretic mobilities, Zetapotential, specific conductivities, viscosities and optimum

plating conditions have been studied as a function of oxide concentration, pH, and temperature. He has shown that increase in temperature and or voltage decreases the particle mobility and hence Zetapotential. The viscosity and conductivity of the various colloidal suspensions increase with an increase of pH and concentration of the suspension. Using suitable conditions coherent, well adhering and uniform plated films were obtained with suspension containing Fe_2O_3, NiO, Cr_2O_3 and TiO_2. The aqueous medium used by Caley contained polyacerylic acid as dispersant and tri-ethylamine as neutralizing base.

1.5 The Choice of Medium

In electrophoresis the electrolyte bath is of great importance. It comprises of particles suspended in a given liquid known as dispersion media. Thus, the selection of media is of particular interest in electrophoretic coating technology.

The choice of suspension medium depends to some extent on the coating problems at hand. As a rule, polar compounds such as alcohols, nitroparaffins and mixtures of these have been found the most satisfactory.

Basically, the desired properties of a suspension vehicle are low viscosity, high density, low electrical

conductivity, high dielectric constant, low evaporation rate, and good chemical stabilty. Low viscosity and high dielectric constant favour a high particle velocity, whereas high density tends to reduce the settling rate. Low electric conductivity (10^{-4} to 10^{-6} mho/cm^2) is necessary to control the secondary electrode effects (gassing and heating). Gassing is undesirable since it damages the deposit, and heating often causes flocculation of the suspension. A low evaporation rate is essential for solvent conservation, and good chemical stability preserves suspension life. Properties of some of the more common dispersing vehicles are shown in Table 1.1.

Table 1.1 Solvent Vehicles

Solvent	Dielectric Constant	Density g/cc	Viscosity, Centipoise
Acetone	21.3	0.792	0.316 (25°C)
Ethanol	25.7	0.793	0.597 (20°C)
Propanol	20.3	0.804	2.26 (15°C)
Isopropanol	18.3	0.786	2.86 (25°C)
Nitromethane	35.8	1.139	0.631 (25°C)
Water		1.00	1.00

Organic liquids have been used as the media since they have higher densities, good chemical stability, low electrical conductivity etc. These media were used early requiring voltages of the order of 2000 volts, since the dielectric constant of the organic solvent is lower than that of water. However, they have been used more frequently than aqueous medium. Again, many organic solvent are toxic in nature and therefore health hazards requiring special handling. They are often expensive. Aqueous solutions are generally expected to be free of aforesaid disadvantages of organic solutions. Accordingly some recent investigations have been directed at deposition from aqueous suspension.[10-12,15].

1.6 Plan of Work

The migration of particles suspended in a liquid medium under an applied potential has been widely investigated, particularly in the paint industry, the field of medicine, and more recently, the automobile industry. Though, general data concerning the motion of fine particles, both in aqueous and organic media is available, the effects of individual parameters, such as pH on a specific system should be investigated before using this data as a base for further study.

A large number of other parameters influence the phenomenon of electrophoresis. These include the physico-chemical nature of the suspended particles being deposited, the nature of the medium, voltage, current etc. Consequently detailed experiments need to be undertaken to assertain the optimum deposition conditions.

Thus, the present work involves the use of electrophoresis in plating various substrates with metal oxide powders from aqueous suspensions. A detailed investigation was carried out in order to obtain optimum coating conditions for a given metal oxide.

Because of this, the present study includes the factors affecting the mobilty and Zetapotential of TiO_2, NiO, Fe_2O_3, Cr_2O_3 and Al_2O_3 powders. Effects of voltage, concentration of the suspension etc. are also considered. The information gathered from these studies is then applied to obtain a condition suitable for plating of iron electrodes with NiO and Cr_2O_3 mixtures. These deposits were further sintered under a reducing atmosphere to obtain a stainless steel composites. A separate study is also made to deposit alumina on graphite rods and plates, which in turn are sintered at high temperatures in an inert atmosphere in order to increase the oxidation resistance of graphite.

CHAPTER 2

THEORETICAL CONSIDERATIONS

This chapter deals with various theoretical concepts involved in explaining the migration of suspended particles in a media under external electric field. Different models of the existence of electric double layer, the concept of zetapotential and mobility of particles with associated parameters are presented in brief.

2.1 The Electrical Double Layer

A colloidal substance is one which is in a fine state of sub-division [3]. In a system where these colloidal substances are suspended in a fluid medium, properties of surfaces and interfaces are important.

The term, 'Electrokinetics' of suspended particles in a suitable medium includes electrophoresis, electro-osmosis, streaming potential and sedimentation potential. The most important of these are electrophoresis, which is the movement of the charged surfaces relative to stationary liquid by an applied field [27] and electro-osmosis, which is the movement of the liquid relative to a stationary surface by an applied electric field.

A property of colloids which, in general, occurs when any two phases come into contact is the establishment of a

potential difference across the interface between the phases. Most substances acquire a surface electric charge when brought in contact with a polar medium. The direction of electrophoresis and its complement, electro-osmosis, are indicated, with reference to a charged solid surface, in Figure 2.1. The picture of electric double layer is shown in Figure 2.2.

2.1.1 Helmholtz Model

Helmholtz in 1879 [4,16] introduced a parallel plate condensor model for the electric double layer, schematically shown in Figure 2.3. It was postulated that to electrically balance the surface charge, oppositely charged ions from solution approach the surface. Thus the double layer consists of two plane layers of charge, the one σ_s on the solid the other σ_L in the solution. This picture of the double layer is analogous to parallel plate condensor.

$$\sigma_s = - \sigma_L = \frac{\varepsilon}{4 \pi \delta} \Psi_o \qquad (2.1)$$

where Ψ_o is the potential across the double layer, ε the appropriate dielectric constant, δ is the distance between the layers. The capacity per unit area, C of the molecular condensor is then given by

$$C = \frac{\sigma_s}{\Psi_o} = \frac{\varepsilon}{4 \pi \delta} \qquad (2.2)$$

This model predicts constant capacity of the double

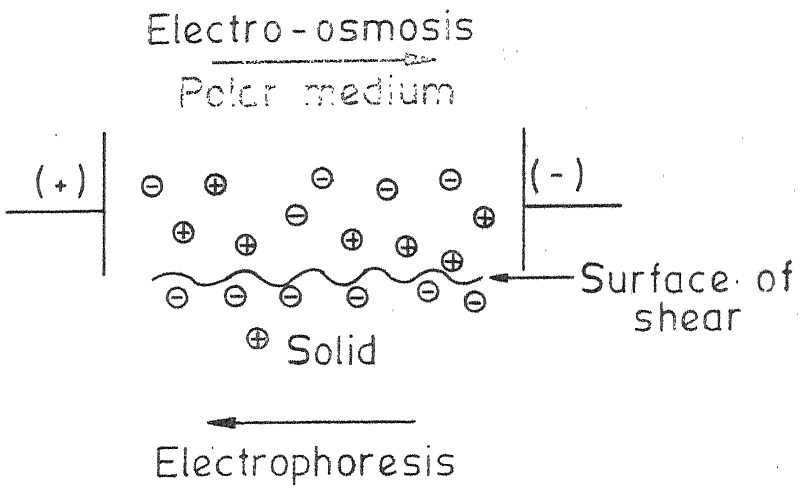

Fig. 2.1 - Electrokinetic phenomena.

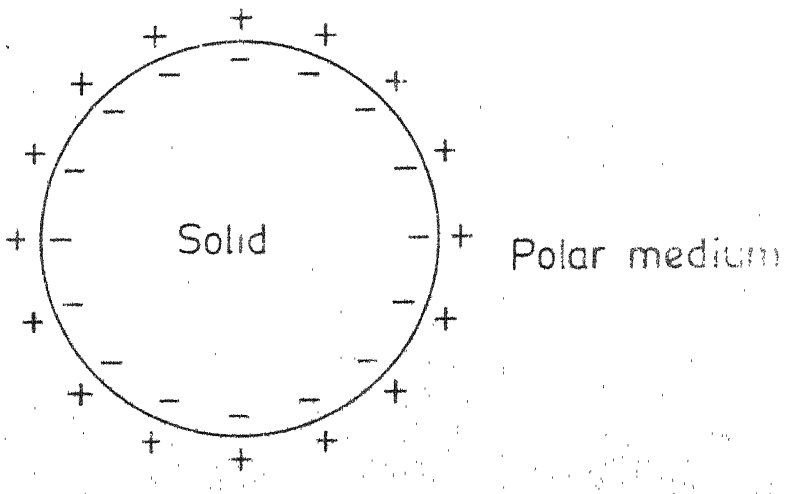

Fig. 2.2 - Schematic diagram of electric double layer

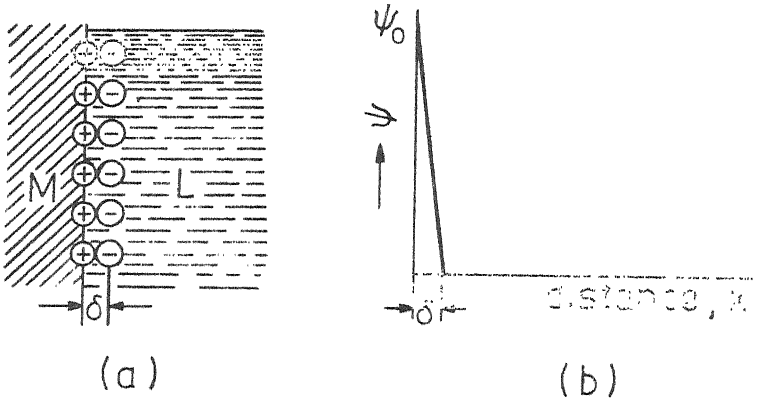

Fig. 2.3 - The Helmholtz model of the double layer (a) molecular picture, (b) variation of potential with distance from the metal - solution interface.

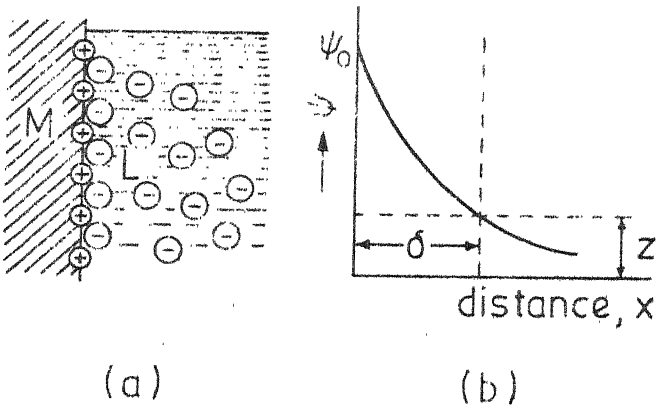

Fig. 2.4 - The Gouy - Chapman diffuse - charge model of the double layer : (a) molecular picture, (b) variation of potential with distance from the metal - solution interface.

layer determined by the size of ions near the surface and is independent of σ_s, Ψ_o and solution concentration - and hence can not be valid in reality.

2.1.2 Gouy-Chapman Model

A more realistic model [9] of the electric double layer was proposed independently by Gouy in 1910 and Chapman in 1913 and is known as the Gouy-Chapman or Diffuse Double Layer model. This model is represented in Figure 2.4.

These authors proposed that ions (in solution), responsible for electroneutrality, diffuse away from the surface because of thermal energy. On the basis of the equations deduced from Gouy-Chapman model [9], it is shown that (a) abnormally large counter-ion concentration near the surface, and (b) abnormally large value of capacitance at potentials from PZC (Point of Zero Charge) exist.

2.1.3 Stern Model

Stern [27] in 1924 proposed an improved model in which the double layer is divided into two regions separated by a plane (stern plane) located about a hydrated ion radius from the surface. The charge distribution on the solution side of the double layer is made up of (i) an ionic layer of charge σ_s lying in a plane parallel to the interface but at a distance δ (of the order of molecular dimension) from it and (ii) the diffuse space charge σ_d of the Gouy-Chapman model.

$$\sigma = -(\sigma_s + \sigma_d) \qquad (2.3)$$

The zetapotential is measured between surface of shear and the diffuse layer, and thus depends on the nature of the mobile part of the double layer. This is schematically illustrated in Figure 2.5.

Stern also called attention to the importance of specific adsorption at the interface. His picture of double layer in the presence of specific adsorption, includes in addition to the smoothed out surface charge, and the diffuse space charge, a layer of specifically adsorbed ions which may exceed in magnitude the charge on the surface and then potential at this layer ψ_δ, may have a sign opposite to that of ψ_o (surface potential).

According to this model the inner region of the double layer, not provided in the Gouy-Chapman model, may be conceived of as a molecular condenser filled with solvent molecules. The fundamental relations of the diffuse layer will still apply provided we substitute ψ_o by ψ_δ in the equation.

The differential capacity C of the double layer is related to C_1, the capacity for inner layer and C_d that for the diffuse layer by the equation

$$\frac{1}{C} = \frac{1}{C_1} + \frac{1}{C_d} \qquad (2.4)$$

$$\therefore \quad C = \frac{d\sigma_s}{d\psi_o} = \frac{d\sigma_s}{d(\psi_o - \psi_\delta) + d\psi_\delta} \qquad (2.5)$$

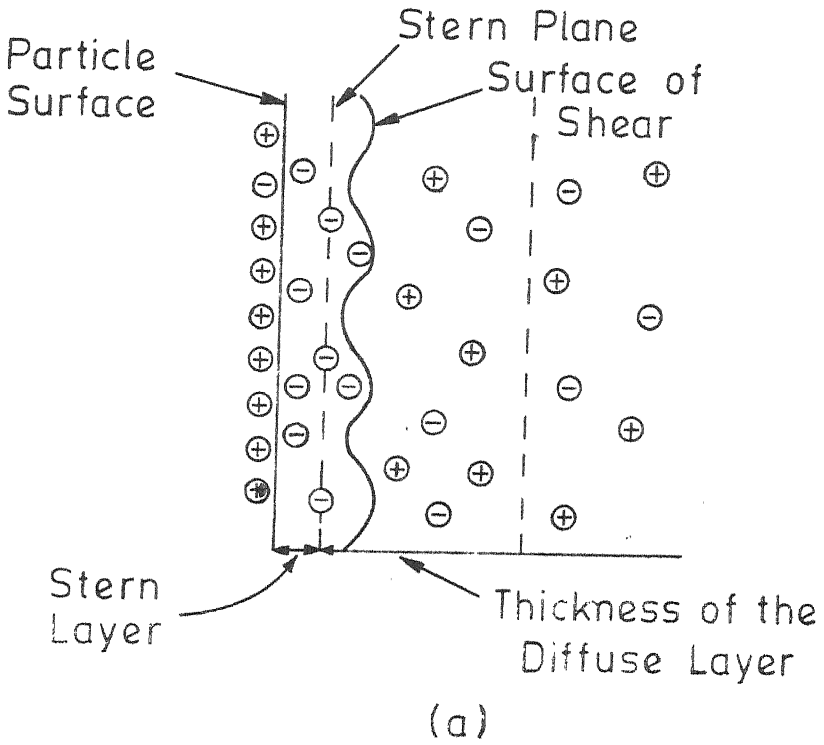

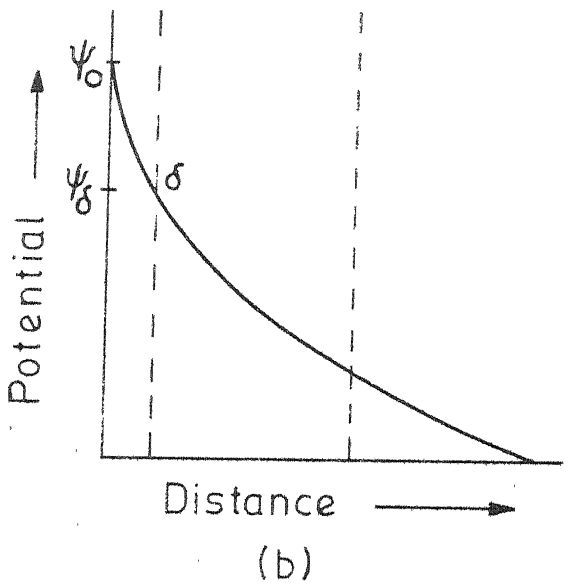

g. 2.5 - Schematic representation of electric double layer according to stern's theory:

(a) molecular picture (b) variation of potential with distance from the solid - liquid interface.

This is equivalent to systems consisting of two condensers in series. According to this model, variation of total C with respect to change in σ_s from PZC, would not be very steep because main change is in C_d and not so much in C_1. The prediction from this theory has better fit (than that of Gouy-Chapman model) with the experimental values.

2.2 Mathematical Analysis of Electric Double Layer

In analysing the electric double layer around a charged particle, two distinct approaches have evolved. In one, the charged particles are considered as point charges and the other deals when the ratio of radius of curvature of the particle to double layer thickness is large. In this case the double layer is treated as being flat.

2.2.1 Flat Double Layer Model: The Smoluchowski equation [2.16]

Consider the motion of the liquid in the diffuse part of the double layer relative to that of non-conducting flat surface. When an electric field ξ is applied parallel to the surface (Figure 2.1), eachlayer of liquid will obtain an uniform velocity which is parallel to the surface. The electrical and viscous forces will balance.

The viscous forces on a liquid layer of unit area, of thickness dx, at a distance x from the surface, and having a bulk charge density ρ may be equated to the electrical force on the same liquid layer. Thus,

$$\xi \cdot \zeta \cdot dx = \left(n \frac{dv}{dx} \right)_{x+dx} - n\left(\frac{dv}{dx} \right)_x$$

$$= \frac{d}{dx} \left(n \frac{dv}{dx} \right) \cdot dx \qquad (2.6)$$

where n = the viscosity of the liquid layer.

The Poisson equation can be written as

$$\zeta = - \frac{1}{4\pi} \frac{d}{dx} \left(\varepsilon \frac{d\Psi}{dx} \right) \qquad (2.7)$$

where ε = the dielectric constant of the medium, and

Ψ = the potential,

Thus; $$- \frac{\xi}{4\pi} \frac{d}{dx} \left(\varepsilon \frac{d\Psi}{dx} \right) = \frac{d}{dx} \left(n \frac{dv}{dx} \right) \qquad (2.8)$$

Integrating equation 2.8

$$\frac{\xi \varepsilon}{4\pi} \left(\frac{d\Psi}{dx} \right) = n \frac{dv}{dx} + \text{const} \qquad (2.9)$$

Now at $x = \infty$, $\frac{d\Psi}{dx} = 0$ and $\frac{dv}{dx} = 0$. Thus, the integration constant = 0. Equation 2.9 may be integrated again giving

$$- \frac{\xi \varepsilon}{4\pi} \Psi = nv + \text{const.} \qquad (2.10)$$

For electrophoresis, the boundary conditions are $\Psi = 0$, $v = 0$ at $x = \infty$ and $\Psi = Z$, $v = v_E$ at the surface of shear, where

v_E = electrophoretic velocity and

Z = the zeta potential.

Therefore,

$$\frac{\xi \varepsilon}{4\pi} Z = n v_E \qquad (2.11)$$

or

$$\mu_E = \frac{v_E}{\xi} = \frac{Z\,\varepsilon}{4\,\pi\,n} \qquad (2.12)$$

where μ_E is in cm sec^{-1}/volt cm^{-1}, Z is in volts, and n is in centipoise. Thus, according to the Smouluchowski equation, the electrophoretic mobility μ_E of a colloid particle of large radius of curvature relative to the double layer thickness in an applied electric field is independent of its size and shape provided that the zeta potential is constant.

2.2.2 Point Charge Model: Huckel Equation

In this model the spherical particle is treated as a point charge. If the spherical particle is large enough for stokes' law to apply, the electrical force on the particle may be equated to the frictional resistance of the medium. Thus,

$$Q_E \xi = 6\,\pi\,n_a\,v_E \qquad (2.13)$$

$$\text{or} \quad \mu_E = \frac{v_E}{\xi} = \frac{Q_E}{6\,\pi\,na} \qquad (2.14)$$

where Q_E = the net charge on the particle (the electrokinetic unit)

ξ = the potential gradient

n = viscosity of the medium

a = particle radius

v_E = electrophoretic velocity

μ_E = electrophoretic mobility.

Now, the zetapotential is the resultant potential at the surface of shear due to charges $+Q_E$ of the electrokinetic unit and $-Q_E$ of the mobile part of the double layer. Thus,

$$Z = \frac{Q_E}{\varepsilon\, a} - \frac{Q_E}{\varepsilon(a + \frac{1}{k})} = \frac{Q_E}{\varepsilon a(HKa)} \qquad (2.15)$$

where ε = the dielectric constantof the electrolytic medium, and Ka = ratio of radius of curvature of particle to the double layer thickness. Since a point was assumed, then Ka is small compared to unity. Therefore,

$$\mu_E = \frac{Z\varepsilon}{6\ \pi\ n} \qquad (2.16)$$

where μ_E is in cm sec^{-1}/volt cm^{-1}, Z is in volts and n is in centipoise. Thus, from these two models prescribed it is evident that the assumed shape of the colloidal particle affects the zeta potential.

2.2.3 Henry Model

A third concept, postulated by Henry [2,3] took into account the conductivity of the two phases. For spheres, the mobility becomes

$$\mu_E = \frac{3K}{2K + K^*}\left(\frac{\varepsilon \zeta}{6\ \pi\ n}\right) \qquad (2.17)$$

where K^* = the conductivity of the colloidal particle and K = the conductivity of the surrounding liquid.

Thus, the expression No. 2.17 reduces to 4π form if $K^* = 0$, and to the 6π form if $K^* = K$. Although there is disagreement concerning the effect of size and shape of colloidal particles on their mobility and Zetapotential, the Smoluchowski equation has been widely used for colloidal systems. Abramson and Michaelis [1], investigated the influence of size and shape on the velocity of long narrow asbestos needles and those of spherical droplets of various oils. The relative velocity of the asbestos needle and the oil droplet was 6.4 and 6.8 respectively. This difference in the mobility is accountable if the effect of particle size and shape is taken into consideration.

2.3 Electrophoretic Deposition

By definition, electrophoresis is only responsible for increasing the local concentration of resin in the vicinity of the anode, and is not involved in any subsequent phenomena.

Anionic substances, which can discharge themselves to the anode, can be listed as:

(i) Simple inorganic anions, arising from extraneous electrolytes which may be present as impurities, catalyst residues etc.

(ii) Particles carrying ionisable, anionic groupings as a part of the polymer chain. Some of these groups will be situated at the surface of the particle and therefore be able to ionise in aqueous phase and give the particle a net negative charge.

The electrolysis of the medium of suspension will also occur simultaneously alongwith the electrophoresis. Electrochemical reactions taking place at the anode and the cathode involves the formation of oxygen and hydrogen respectively. This further complicates the understanding of system.

According to the Finn and Mell [14] the film deposition is largely dependent on coagulation of the polymer solids at the anode through the formation of insoluble metal cations produced by the electrolysis of the anode itself. Thus, a zone of low pH is produced around the anode by the discharge

of hydroxyl ions to produce molecular oxygen and hydrogen ions. The resin is then precipitated in the form of the unionized acid on metals, ions leaving the anode will interact with the resin to give insoluble salts.

However, according to Tawn and Berry [30] there are two mechanisms leading to the precipitation of the resin. The main process is the production of hydrogen ions which neutralize the resin anions, and precipitate the resin in acid form, while a secondary process involves the dissolution of the anode metal, thereby producing insoluble metal salts.

Further theories [25] involve neutralization of the resin in the double layer before deposition, leaving the repelled water dipoles behind as components of the double layer.

As can be seen, there is much disagreement concerning the mechanism involved in the coagulating of the resin at the anode.

CHAPTER 3

ELECTROPHORETIC TRANSPORT PROPERTIES AND DEPOSITION OF THE METALLIC OXIDES TiO_2, NiO, Cr_2O_3, Fe_2O_3 AND Al_2O_3 IN AQUEOUS SUSPENSIONS

The effect of pH and solid concentration on mobility, zetapotential, specific conductivity and viscosity of aqueous suspension is considered in this chapter. Determination of optimum plating condition, for deposition of oxides TiO_2 and Al_2O_3 is also included.

3.1 Electrophoretic Transport of Metal Oxides:

3.1.1 Introduction

The study of mobility and zetapotential with respect to pH of TiO_2, NiO, Cr_2O_3, Fe_2O_3 and Al_2O_3 has been undertaken to determine the relationship between these parameters and plating characteristics of the oxides.

As a rule, oxide powders such as TiO_2 and Al_2O_3 are not dispersed into their individual particles in a suspension [10]. The size of aggregates present is dependent on the concentration of the powder, the dispersing liquid, the dispersing agent, and pH. Thus, before mobility studies can be undertaken, the particles of interest must be satisfactorily dispersed. An aqueous dispersing medium was chosen for the present study, because of the advantages of using aqueous

baths for electrodeposition. The use of electrophoresis in plating processes are normally based on the use of organic dispersing media, such as isopropanol or nitromethane [15] which have a number of disadvantages including the fire hazard when using large volumes and voltage in the process.

It is therefore, necessary to obtain a dispersing agent which, when added to the aqueous-oxide powder bath, would result in a stable suspension. Many such agents are available, including viscous oils, alkyd resin, melamine, and acrylics [10]. Use of waxes, ureaformaldehyde resin and shellac has also been reported [10]. For the present study many such reagents were tried viz. sodiumpyrophosphate, aluminium nitrate, sodium silicate and polyacrylic acid. Out of these, a polyacrylic acid, acrysol A-5 was found satisfactory, and was used throughout the experiments. Acrysol acts as a dispersent (activator) and a binder as well.

The various methods [16] of measurement of the velocity of electrophoresis of moving particle can broadly be classified into two categories, microscopic and macroscopic. In the microscopic method an individual particle in motion under an applied potential is studied whereas, the movement of the bulk suspension can be considered in the macroscopic which is also known as moving boundary electrophoresis technique. Although the microscopic procedure has several advantages,

in the respect of simplicity, time required and information it gives concerning the size, shape and orientation of the particles, the macroscopic method considers the movement of the bulk suspension which is of more interest in plating from such suspensions.

In plating on a given substrate, the film thickness (or weight), as well as the water content of the film have a decided effect on the quality of the resulting plate. Thus, care must be taken to predetermine these factors. Parameters such as viscosity and conductivity of a given suspension are only indirectly related to the resulting film quality and hence are determined.

It has been reported [12] that the films of TiO_2 obtained exhibited a great deal of rupture, due to the escape of trapped gases. This occurrence was removed by obtaining a suitable plating voltage, time, suspension concentration and size of the powder particles.

Tawn and Berry [30] noticed that there was no change in the coulombic yield with concentration for these oxides. In most cases there was an increase in coulombic yield, as well as coating deposited with an increase in concentration, as reported by Caley [10].

3.1.2 Experimental Materials

Polyacrylic acid, acrysol A-5 was obtained from Rohm and Haas Company, Philadelphia (U.S.A.). Some of the properties are listed in Table 3.1. The Fig. 3.1 shows the effect of pH variation of deionized water by adding acrysol. pH decreases with addition of acrysol.

TABLE 3.1

Physical Properties of Acrysol A-5

Polymer concentration	25 percent
pH (5 percent aqueous solution)	approx. 2
Dissolution with water	Infinite
Molecular weight	Less than 300,000
Brookfield viscosity	
5 Percent concentration	20 cps
25 Percent concentration	18,000 cps

Deionised water (D.I. water) was prepared in I.A.C. water plant using mixed bed resin demineralizer. The specific conductivity of D.I. water was between 0.5 to 1.0 micromhos.

The oxides viz., TiO_2, NiO, Cr_2O_3, Fe_2O_3 and Al_2O_3 were mostly analytical reagent quality. The particle size was made to control within 10μ by wet grinding. Table 3.2 shows the grade, supplier, density values etc. of the powder concerned.

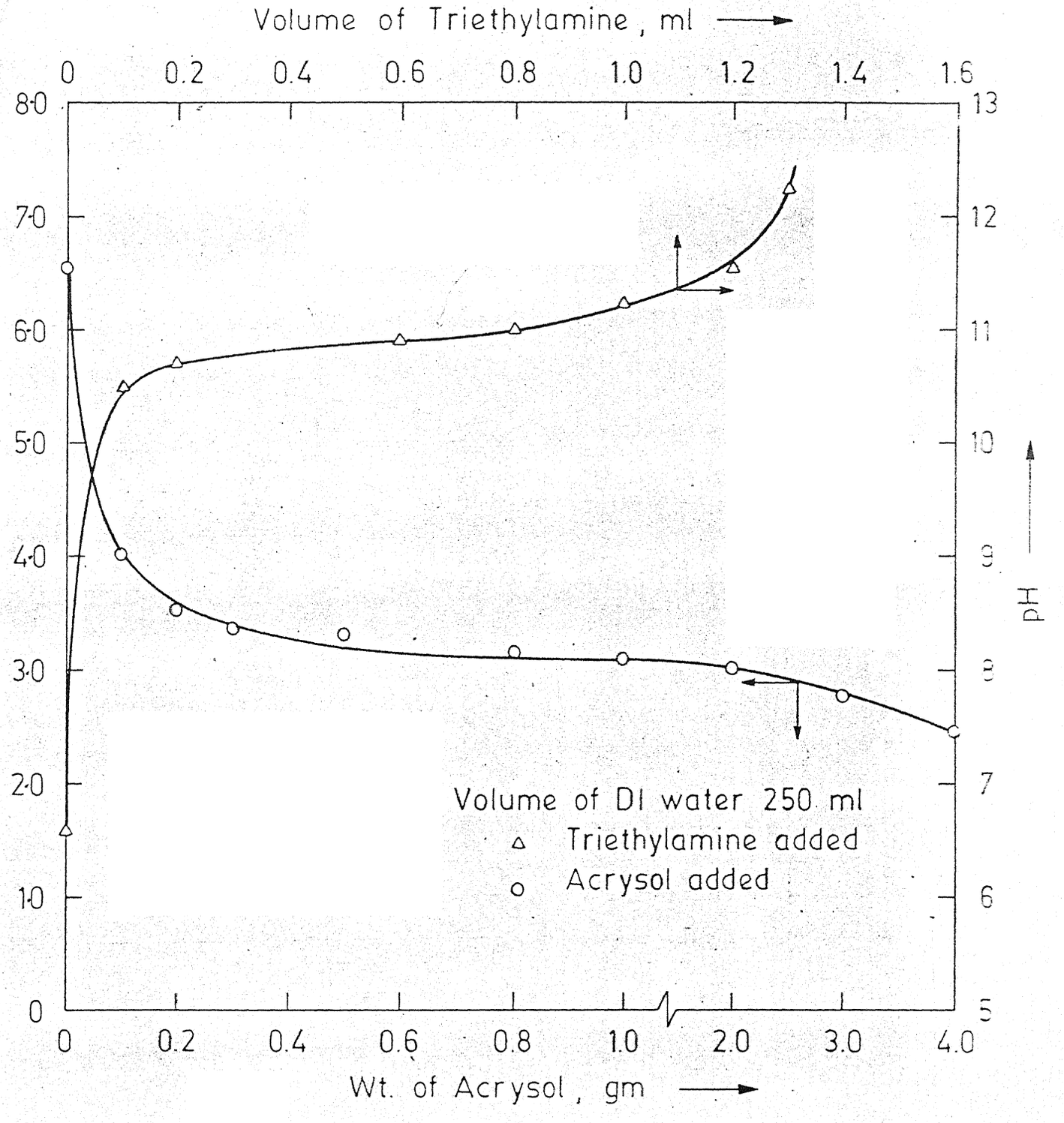

Fig. 3.1 - Variation of pH with Acrysol and Triethylamine.

TABLE 3.1

Details of Various Oxide Samples

Sample	Formula	Grade	Colour	Specific gravity	Supplier
Titanium dioxide	TiO_2	LR	Colourless	4.26	B and B Company Ltd. Bombay (India)
Iron Oxide	Fe_2O_3	AR	Brown	5.12	Fischer Scientific Corp. (USA).
Nickel Oxide	NiO (N1)	AR	Grey	7.45	-do-
Nickelous Oxide	NiO (N2)	AR	Grey		-do-
Nickel Oxide	NiO (N3)	LR	Black		B and B Company Ltd. Bombay (India).
Chromium Oxide	Cr_2O_3	AR	Green	5.21	Fischer Scientific Corp. (U.S.A.)
Alumina	Al_2O_3(A1)	AR	Colourless	3.99	Alcoa Ltd.,USA
Alumina	Al_2O_3(A2)	AR	Colourless		-do-

Triethylamine was obtained from S.M. Chemicals, Baroda (Gujrat). Figure 3.1 also includes the effect of pH variation of deionized water by adding triethylamine (TEA).

Procedure:

To determine the specific conductivity and viscosity of oxide, aqueous suspensions at three powder weight concentrations (PWC) 3.2 per cent, 4.0 per cent and 4.8 per cent were prepared by a high speed mechanical stirrer. To each of these suspensions, polyacrylic acid (dispersant), was added in the ratio of eight weight parts powder to one weight part dispersant. This fixed powder to dispersant ratio was used in all the experiments which gave most stable suspensions. An increase in the dispersant causes floculation while decrease resulted in an unstable suspension.

Because of polyacrylic acid addition the suspension was acidic. The pH varied from 3.6 for 3.2 per cent PWC to 3.4 for 4.8 per cent PWC. From this point the pH was adjusted upto 11 by addition of an organic base, triethylamine $[C_2H_5]_3N$ to the suspension.

Similarly, in mobility measurements, for each oxide studied, 100 ml. of aqueous suspension at concentration 0.1 per cent PWC was prepared and 0.4 g of polyacrylic acid was added. These additives were kept constant for all these experiments. Adjustment of the pH from this point to a higher value was again restored by addition of triethylamine.

Thus, the pH range covered was from 3.4 to 11. The suspension were allowed to remain overnight in sealed plastic containers before any mobility measurements were being made.

The specific conductivity was measured with Direct-current Specific conductivity meter Type 303, S.No.11, supplied by Systronics Co. Ltd., Ahemadabad (India).

The viscosity measurements were made by a rotating type viscometer, Rheotest -2 (made in West Germany).

For mobility measurements, zetameter (Zetameter Inc., New York, U.S.A.) was used. The runs in the electrophoretic cell were made by using prescribed voltages [33] depending upon the conductivity of the suspension at room temperature and at various pH levels. The electrophoresis cell is shown in Figure 3.2. The suspension to be studied was introduced in the cell, taking precaution that no air bubble was entrapped The power source of the zetameter consisted of constant voltage/constant current unit, with a maximum output of 300 volts. Platinum anode and Platinum-Iridium cathode were plugged on top of each arm of the cell.

At first the conductivity of the suspension was measured by the unit attached to the instrument and accordingly the suitable voltage was applied for the electrophoresis. The cell was illuminated by a lamp source and the particles were focussed thru' the microscope using 10x eyepiece and 6x as objective. The time taken by the particles to cover a

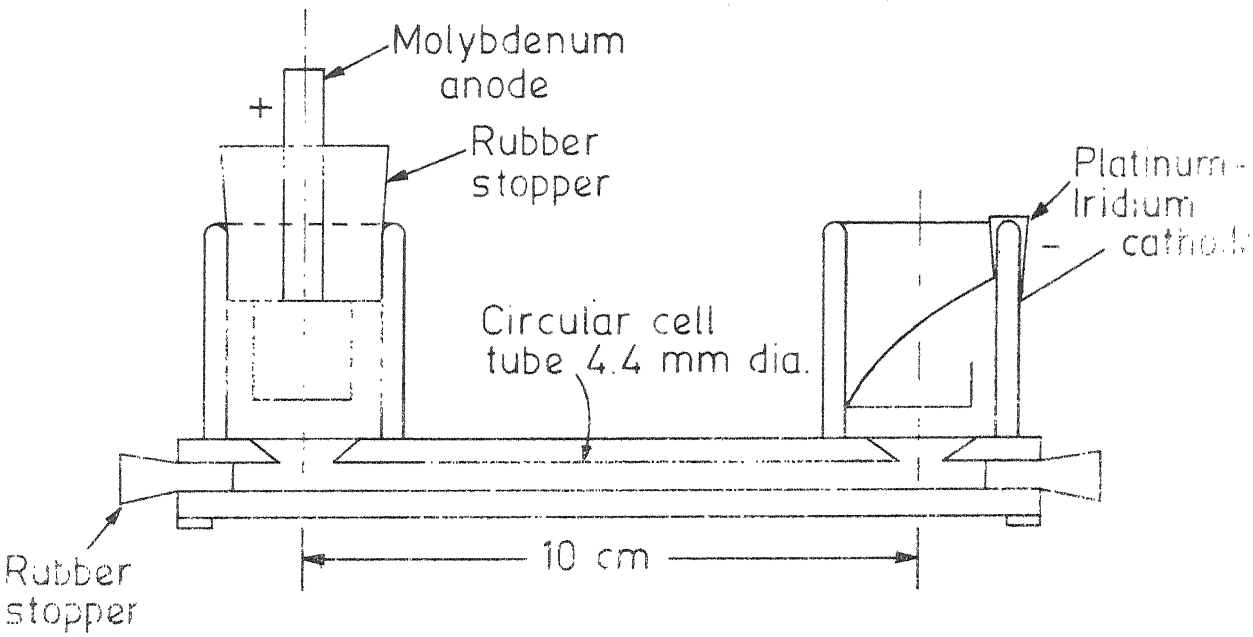

Fig 3.2 - Electrophoresis cell to measure mobility.

unit distance was measured by the help of timmer. The average time was taken after fifty such observations. Similarly it was followed for all other pH levels. The mobility and zetapotential values were thus obtained using Henry-Smoluchowski formula from the tables provided by the supplier of the instrument.

3.1.3 Results and Discussions

Relationship between pH, Specific Conducitivity, Viscosity and PWC.

Typical pH-conductivity and pH viscosity curves for Al_2O_3 are given in Figure 3.3 and Figure 3.4 respectively. From the Figure 3.3 it is seen that specific conductivity increases with pH. Further, an increase in PWC results in a greater conductivity at constant pH.

From Figure 3.4, an increase in viscosity with an increase in pH is also apparent for the same PWC. The remaining oxides also give similar pH-conductivity and pH-viscosity profiles. However, PWC has an effect on both.

Mobility-pH Profiles for TiO_2 and Other Oxides:

The mobility pH profiles for TiO_2 are shown in Figure 3.5. The pH is varied by sets of addition viz. HCl-NaOH and poly-acrylic acid-triethylamine. From the Figure 3.5 it can be seen that the mobility of TiO_2 appear to reach maximum at pH range 6.5 to 7.2 in both the cases. This also shows that

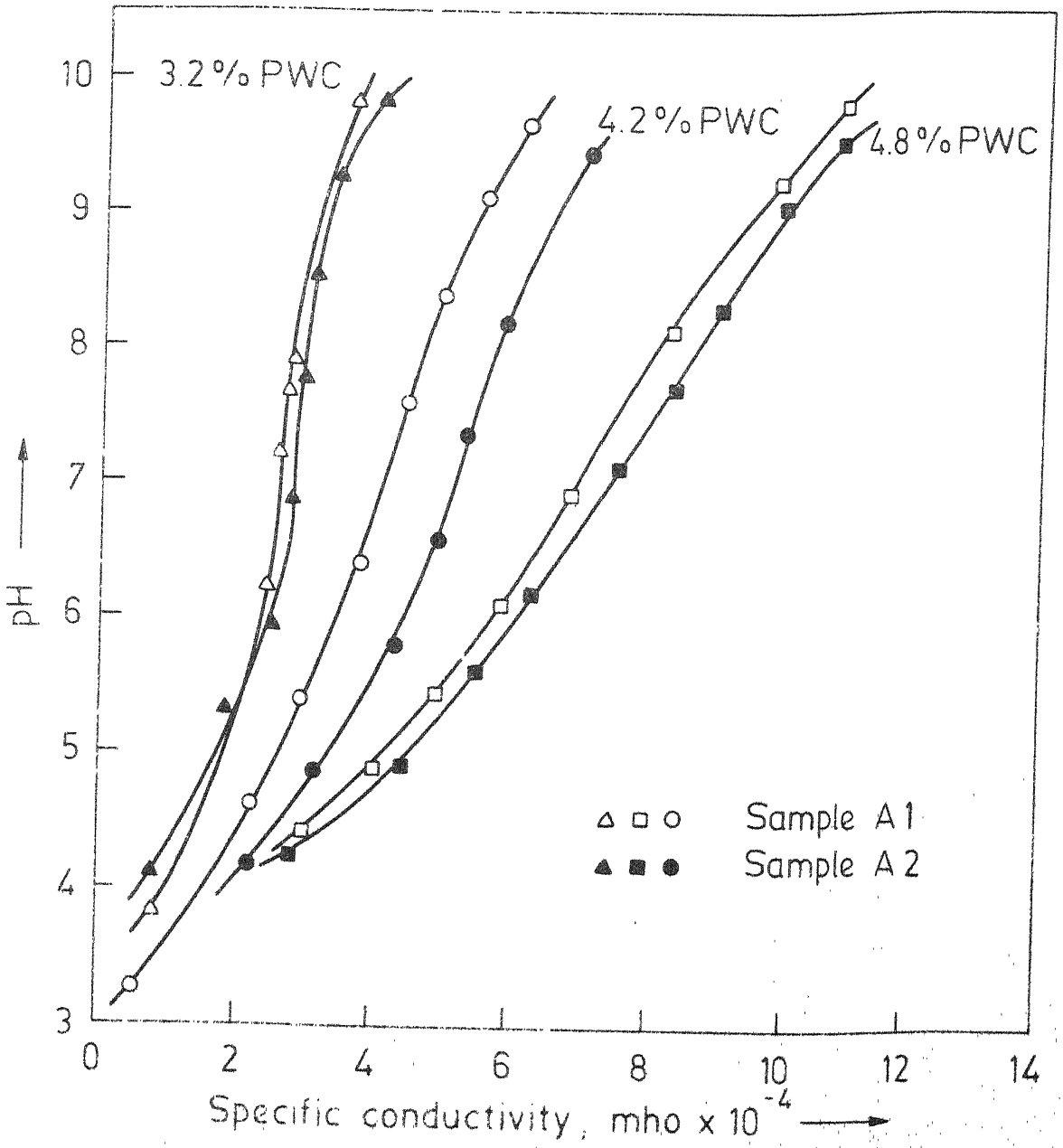

Fig 3.3 - Graph of pH dependence on conductivity for Al_2O_3.

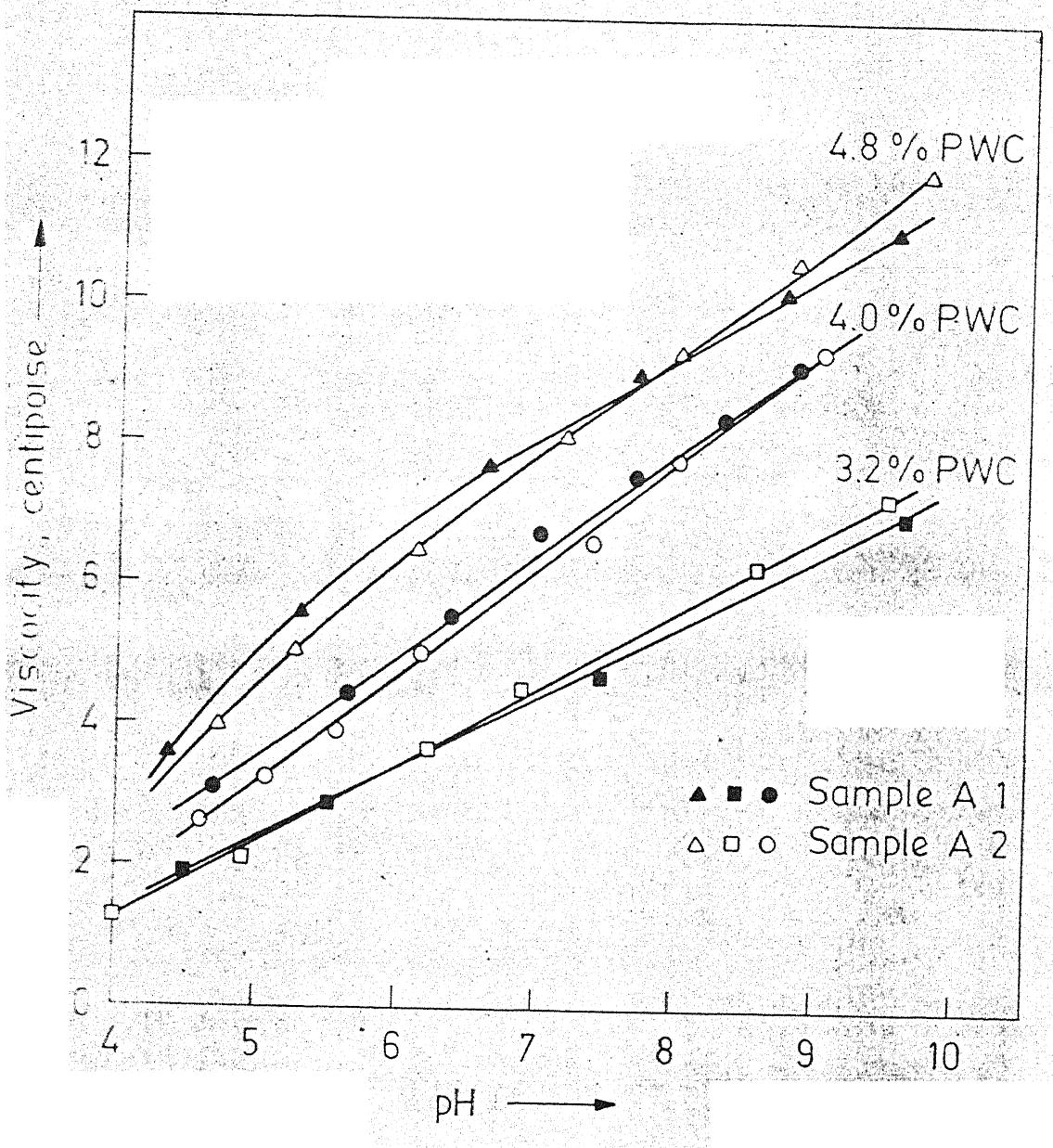

4 - Graph of pH dependence on viscocity for Al_2O_3 samples.

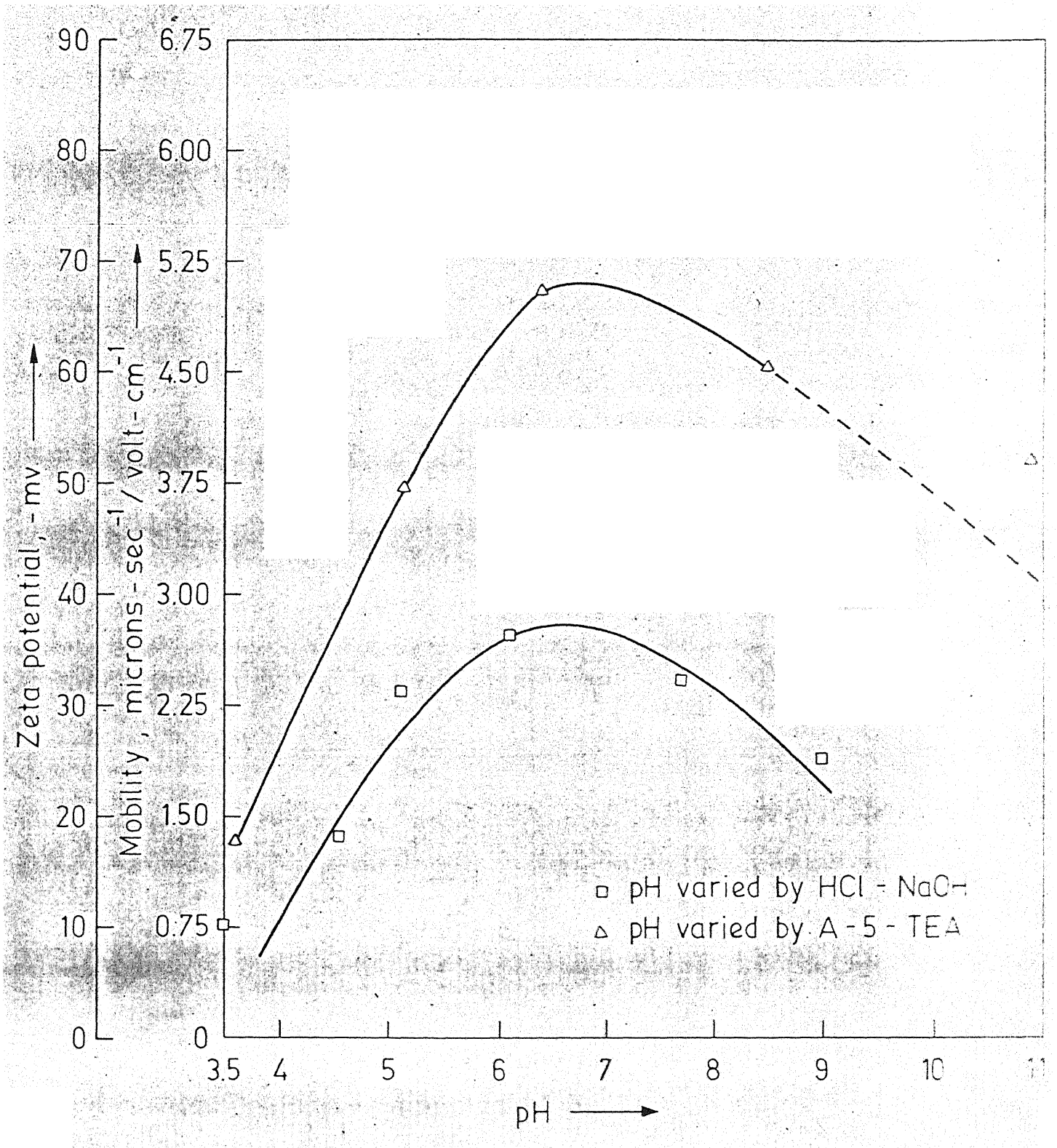

Fig. 3.5 - Graph of mobility and zeta potential vs pH profiles for TiO_2

the addition of polyacrylic acid-triethylamine increases the mobilityof the particles as compared to the addition of HCl-NaO

The behaviour of three different nickel oxides are shown in Figure 3.6. Sample N1 and N2 show continuous increase in the mobility from pH 3, reaches maximum at about pH 6.5 and then decreases continuously with pH. This behaviour is similar to that of TiO_2 (Figure 3.5). The sample N3 behaves differently from the first two. With sample N2, the mobility continuously increases with pH.

The variation in the behaviour of mobility with pH of these samples is attributed to the fact that these oxides have different surface characteristics.

Figure 3.7 shows mobility of Cr_2O_3 and Fe_2O_3 with pH. The mobility of Cr_2O_3 and Fe_2O_3 increases with pH, reaches maximum of about 3.13 and 5.32 microns sec^{-1}/volt cm^{-1} respectively and then decrease with pH. Cr_2O_3 peaks at pH 6.5 whereas, Fe_2O_3 at about pH 7.0.

Alumina is stable in acidic as well as basic medium. It forms a stable suspension at pH lower than 2 and pH higher than 7.00. The stability however increases with pH beyond 7.0. The behaviour of mobility with pH for two alumina samples A1 and A2 is shown in Figure 3.8. These two samples, A1 and A2, show continuous increase in the mobility in the pH range from 4 to 10.

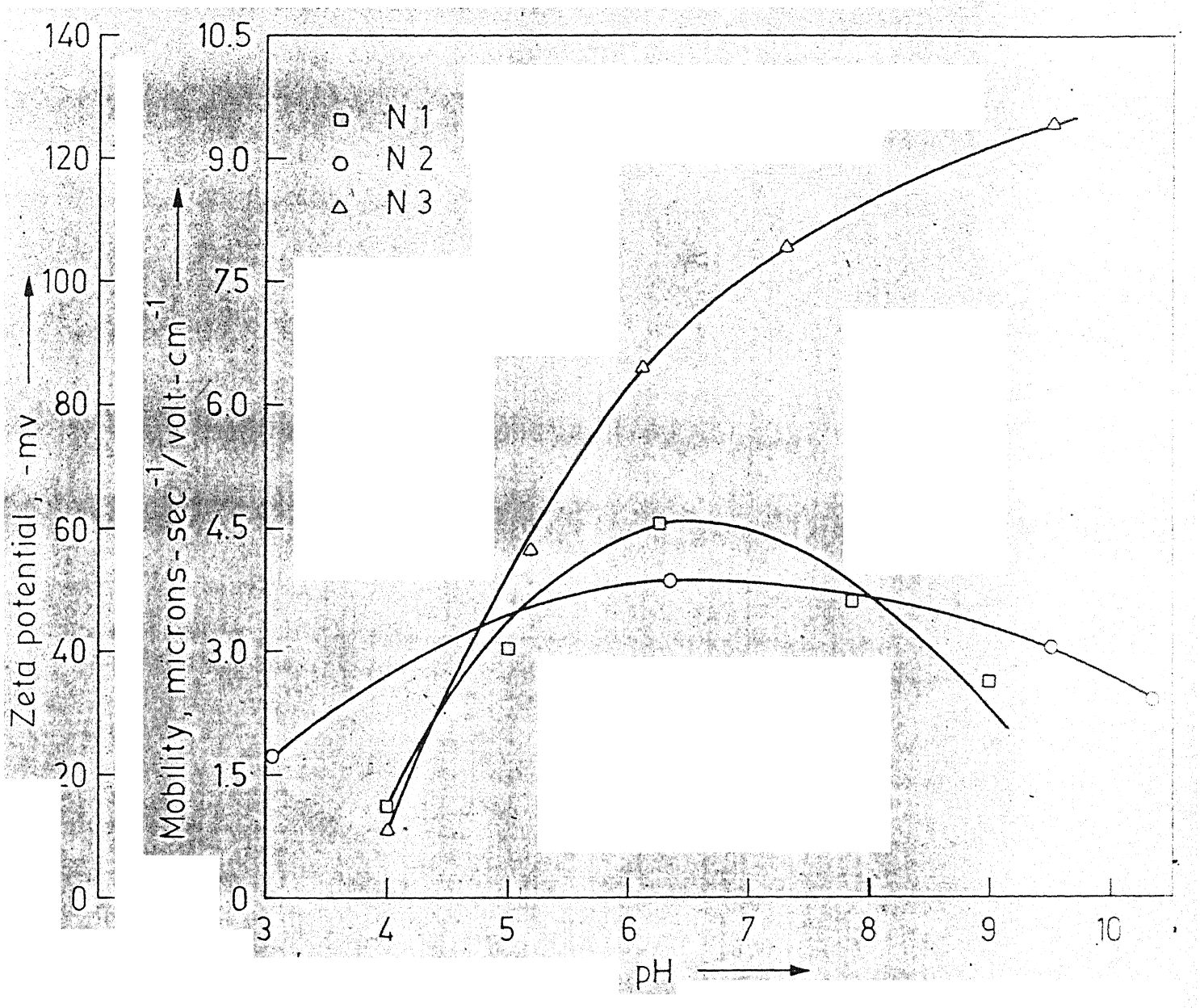

Fig. 3.6 - Graph of mobility and zeta potential vs pH for three different samples of NiO.

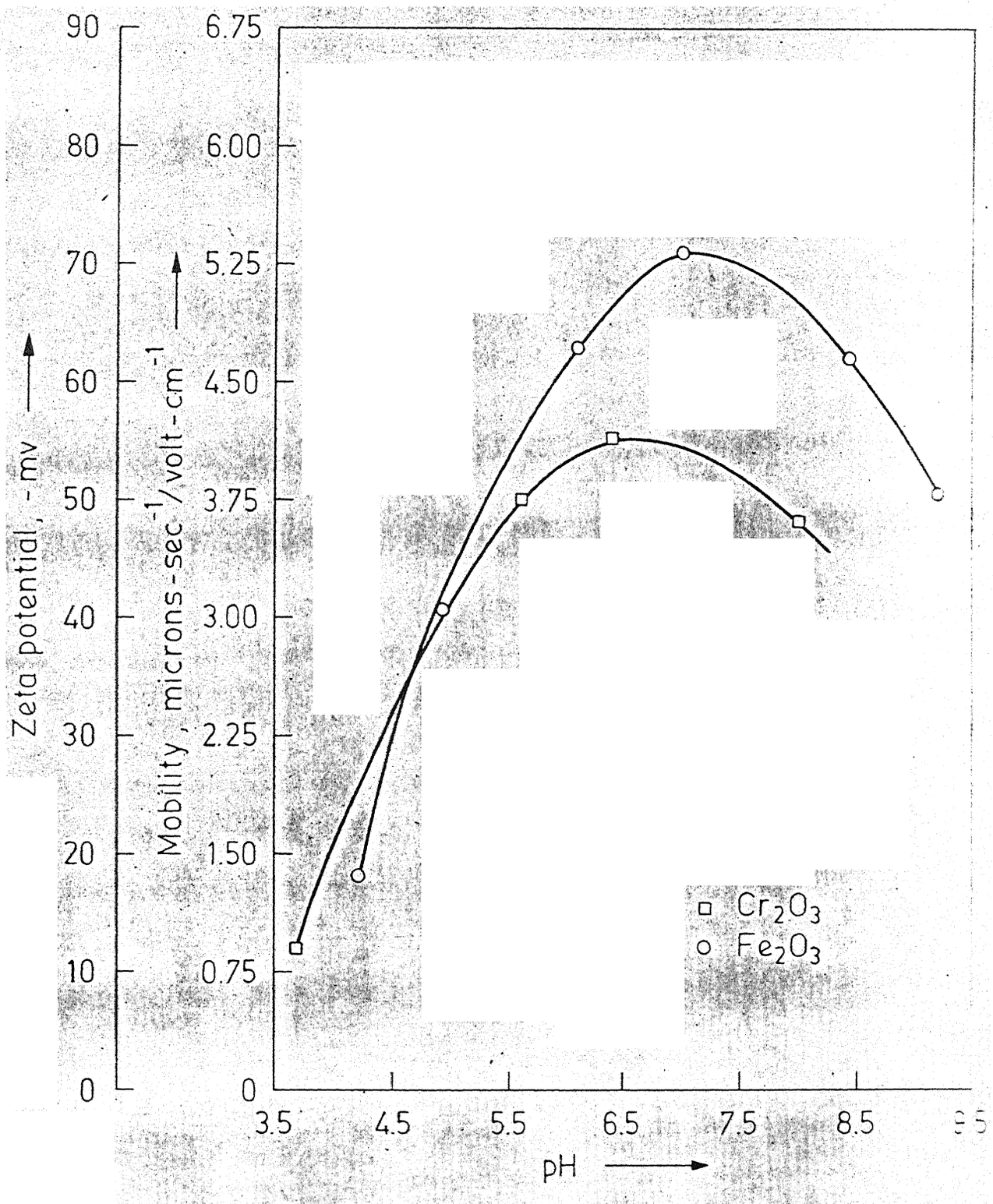

Fig. 3.7 - Graph of mobility and zeta potential vs pH for Cr_2O_3 and Fe_2O_3.

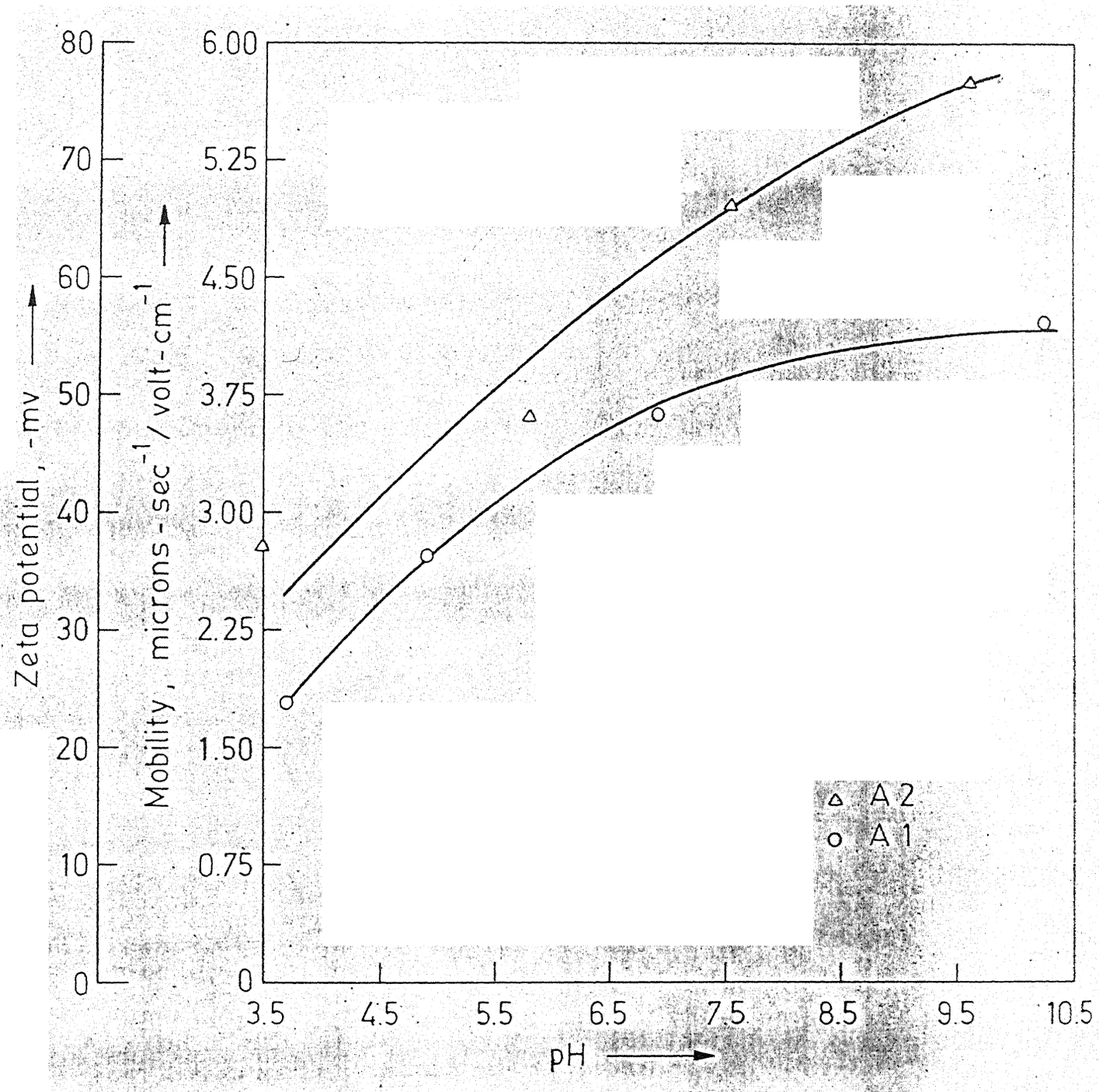

Fig. 3.8 - Graph of mobility and zeta potential vs pH for Al_2O_3.

It was felt imperative to examine the change in mobility pattern of suspended particles when their surfaces are modified by a suitable technique. This was done for Al_2O_3 (sample A2) by activating [19] it by an aqueous solution of $TiCl_3$ (15 per cent). 10g of Al_2O_3 was mixed with 10 ml of $TiCl_3$ for about 15 minutes. The excess $TiCl_3$ was removed. This mixture was kept at 45°C under vacuum for 24 hours. It was then thoroughly washed with distilled water and dried. Thus, the surface of alumina was activated which is schematically shown below

$$Al_2O_3 \xrightarrow[TiCl_3(15\ per\ cent)]{Activated} Al\begin{matrix}OH\\OH\end{matrix}Ti \qquad (3.1)$$

(A-2) (A-2 S)

The results of mobility measurements of A-2 and A-2S are compared in Figure 3.9. It can be seen that the mobility of the activated sample initially increases with pH 3.8, reaches maximum at pH 8.5 and then decreases with pH. This behaviour as expected is similar to TiO_2 case, except the peak value of pH is different.

The mobilities resulting from different surface treatments have different values [10], although it has been reported that inspite of the varying nature of dispersed particles, the electrophoretic mobilities for aqueous solutions always lie within the range of 2 to 4 x 10^{-4} cm sec^{-1}/volt.cm^{-1}[17].

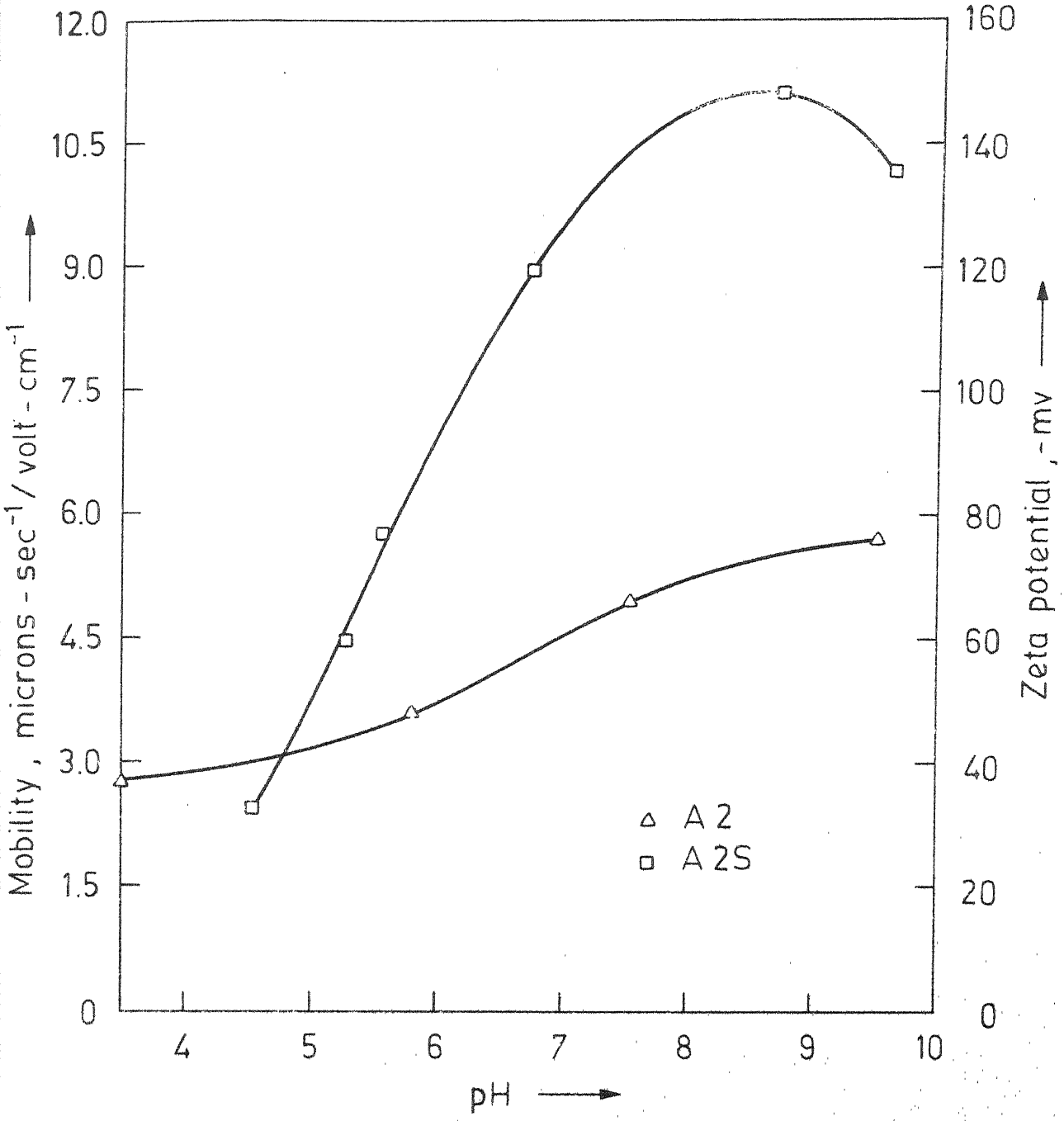

Fig. 3.9 - Graph of mobility , zeta potential - pH for Al_2O_3 .

The mobilities in the present work were generally in agreement in the range given by Glasstone [17].

Zetapotential-pH Profiles for Oxides

The mobility-pH profiles are parallel to zetapotential profiles. This is expected as the mobility and zetapotential are interrelated through Smoluchowski equation as given below

$$Z = \frac{4 \pi \mu n}{\varepsilon} \qquad (3.2)$$

Here the dielectric constant ε and factor 4π represents a constant for each oxide concern. Thus, the only dependent variable for the mobility is viscosity. The viscosity was shown in the Figure to vary almost linearly with pH. Thus, mobility pH profiles and zetapotential- pH profiles are expected parallel in behaviour.

The corresponding behaviour and values of zetapotential with respect to pH are also shown in Figures 3.5 to 3.9.

The values of the zetapotential were also in agreement in the range given by Glasstone [17]. From Alexander [3] and data concerning rutile pigments, a common zetapotential range is 25 to 60 mv. However, it has been noted that adsorbed surfactants or other additives may raise the zeta-potential to 250 mV or more.

Summary

SUMMARY

The effect of PWC, viscosity, pH and surface characteristic on particle mobility and zetapotential has been presented with reference to TiO_2, Fe_2O_3, NiO, Cr_2O_3 and Al_2O_3.

The viscosity and conductivity of the various colloidal suspensions prepared was found to increase with an increase in pH. There was also a noticable dependence of these two parameters on PWC, a greater PWC resulting in a greater conductivity and viscosity at a given pH level.

The behaviour of pH-mobility and pH-zeta-potential profiles depends upon the surface characteristics. The oxides TiO_2, Cr_2O_3, NiO and Fe_2O_3 exhibited similar pH-mobility and pH-zetapotential curves, each approaching a maximum mobility and zetapotential. The oxides like Al_2O_3 have not shown this type of trend.

3.2 Determination of Optimum Plating Conditions:

3.2.1 Introduction

The deposition of smooth, uniform and coherent films using electrophoresis is considered with reference to the factors affecting the quality of the deposits. Holzinger [20, 21] has investigated the effect of pH and bath agitation on coulombic efficiency, which in turn related to the weight of the film deposited. The pH was found to change continuously during the deposition. The increase in pH is thought to be the formation of OH^- at the cathode, and thus the bath must always be checked since optimal coating is only achieved in a narrow pH range. Bath agitation was found to decrease the coulomb efficiency [20] with rapid stirring, tending to striate the films.

3.2.2 Experimental

For each of the oxides taken for the present investigation, coating conditions such as voltage, time of deposition, pH of the suspension and suspension concentration was undertaken. Deposition times from 30 sec to 180 secs were investigated at voltages ranging from 10 v to 70 v. A wide range of pH from 6.0 to 10 was used. In some cases mobility peaks at certain pH values in the mobility vs pH profiles. This peak value of pH was therefore, used in case of TiO_2, NiO and Cr_2O_3. For each case, the electrode on which

the film was to be deposited, was placed between two cathodes of equal size, each at a distance of 3.4 cm. from the anode. The electrodes were rectangular in shape, cathodes being 6.55 cm x 5.55 cm, and anode being 3.5 cm x 3 cm. The thickness of both, anode and cathode material was 0.6 mm. Cathode material was 18:8 stainless steel and anode was mildsteel containing 98.75 per cent Fe. The anodes were numbered to avoid any confusion.

The apparatus for deposition is shown in Figure 3.10 and the circuit diagram in Figure 3.11. The suspension was slightly agitated before a run and not during a run, so that no unnecessary variables were introduced.

Each electrode was washed in 8 per cent orthophosphoric acid solution for 5 min. at 70°C, then thoroughly rinsed in distilled water, deionized water and then acetone. The plates were handled by inserting a suitable wire through a small hole drilled at the top of each plate to avoid contamination.

3.2.3 Results and Discussions

Preliminary Measurements

Since the electrophoresis is extremely sensitive to the electrolytic medium, some preliminary experiments were carried out to examine the nature of deionized water. Using the electrode arrangement (Figure 3.10), current vs potential

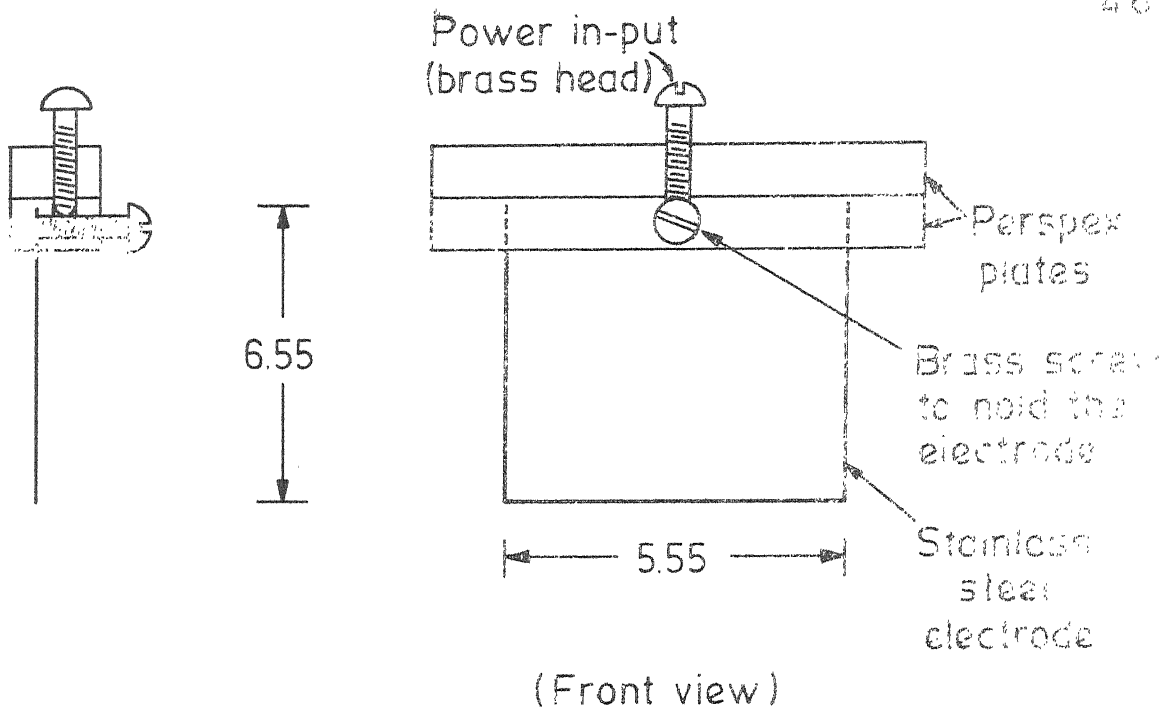

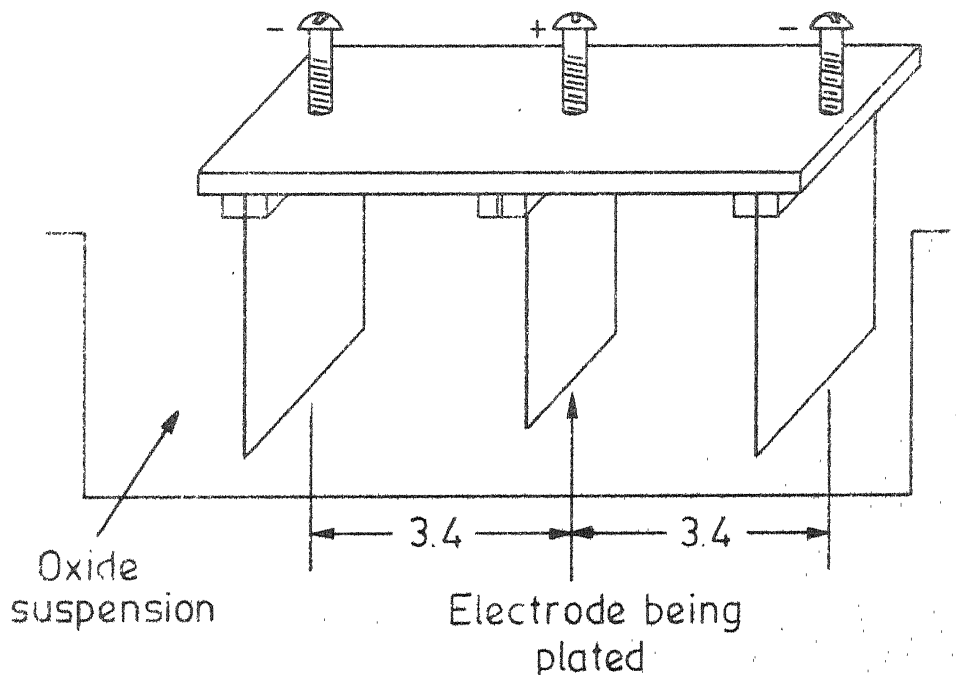

Dimensions in cms.

Fig. 3.10 - Electrophoretic cell arrangement for deposition on rectangular electrodes.

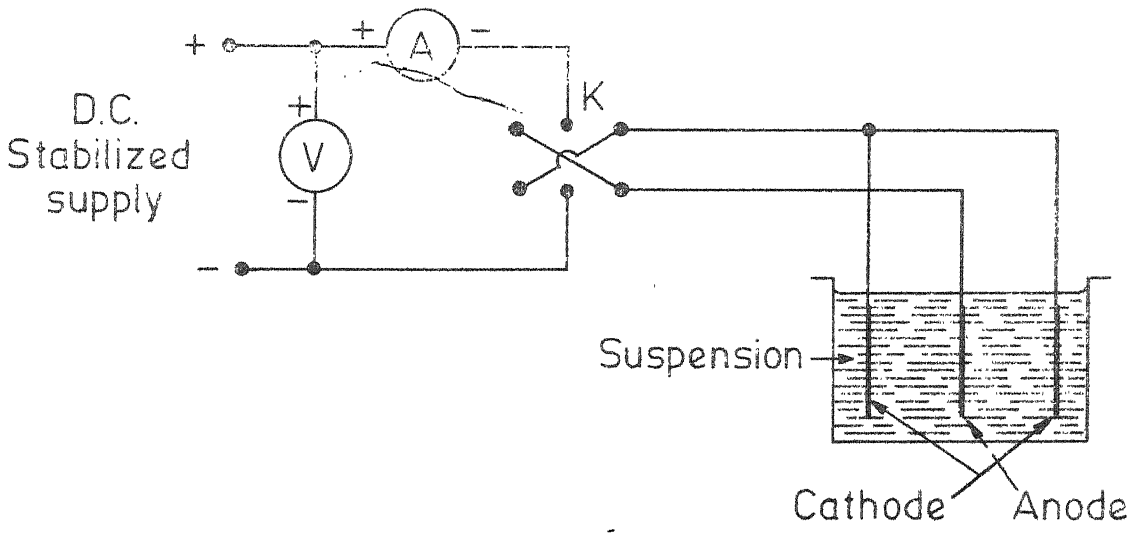

Fig 3.11 - Circuit diagram for electrophoretic deposition.

graphs were obtained for D.I. water. For comparison purposes, similar profiles were obtained with distilled and double distilled water. Figure 3.12 shows that at the same potential, the current decreases as the purity of the water increases. In this case the current is least for D.I. water and higher for distilled water at the same voltage.

Figure 3.13 shows that the current generally increases with time. Large conductivity of electrolyte is undesirable for electrophoretic deposition due to larger IR losses and gas evolution at electrodes. The gradual increase in the current and thus, the conductivity of water with increased time of exposure is possibly due to dissolution of CO_2 from air to form CO_3^{2+} and HCO_3^- ions. in solution. This is substantiated by the observation that the conductivity values are restored to original values when an inert gas like Ar or N_2 is bubbled through the solution. The Figure 3.14 shows the bubbling arrangement. It has been observed that while it is difficult to get electrophoretic deposition from suspensions in 'degenerated water', good deposits can however, be obtained again by bubbling Ar.

Deposition of TiO_2

In determination of deposition time and voltage, the effect of both high voltage and long deposition times was found to be detrimental to the resulting film. That is, the film of TiO_2 badly cracked upon drying, and subsequently peeled

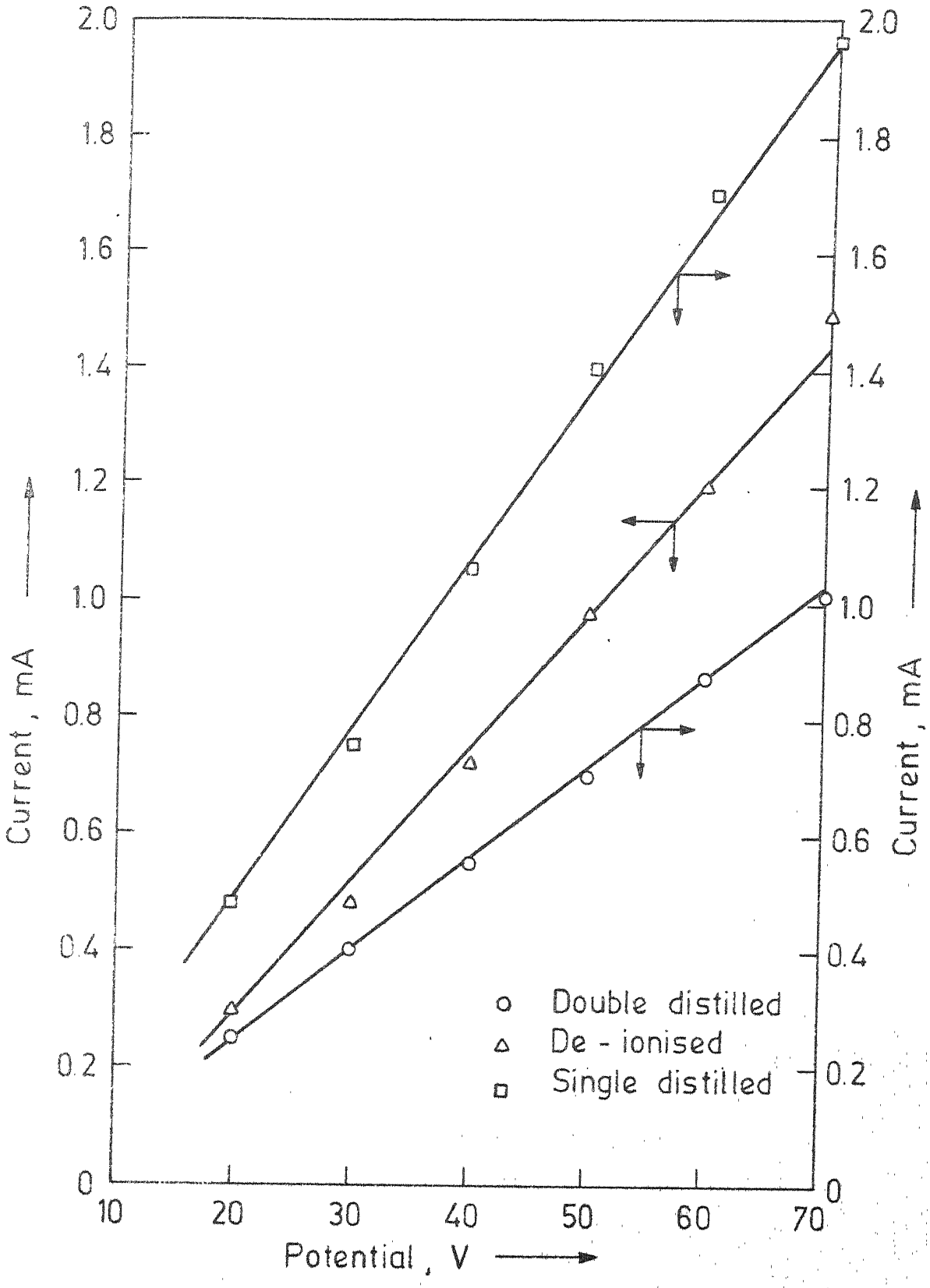

Fig. 3.12 - Potential - current curves for water

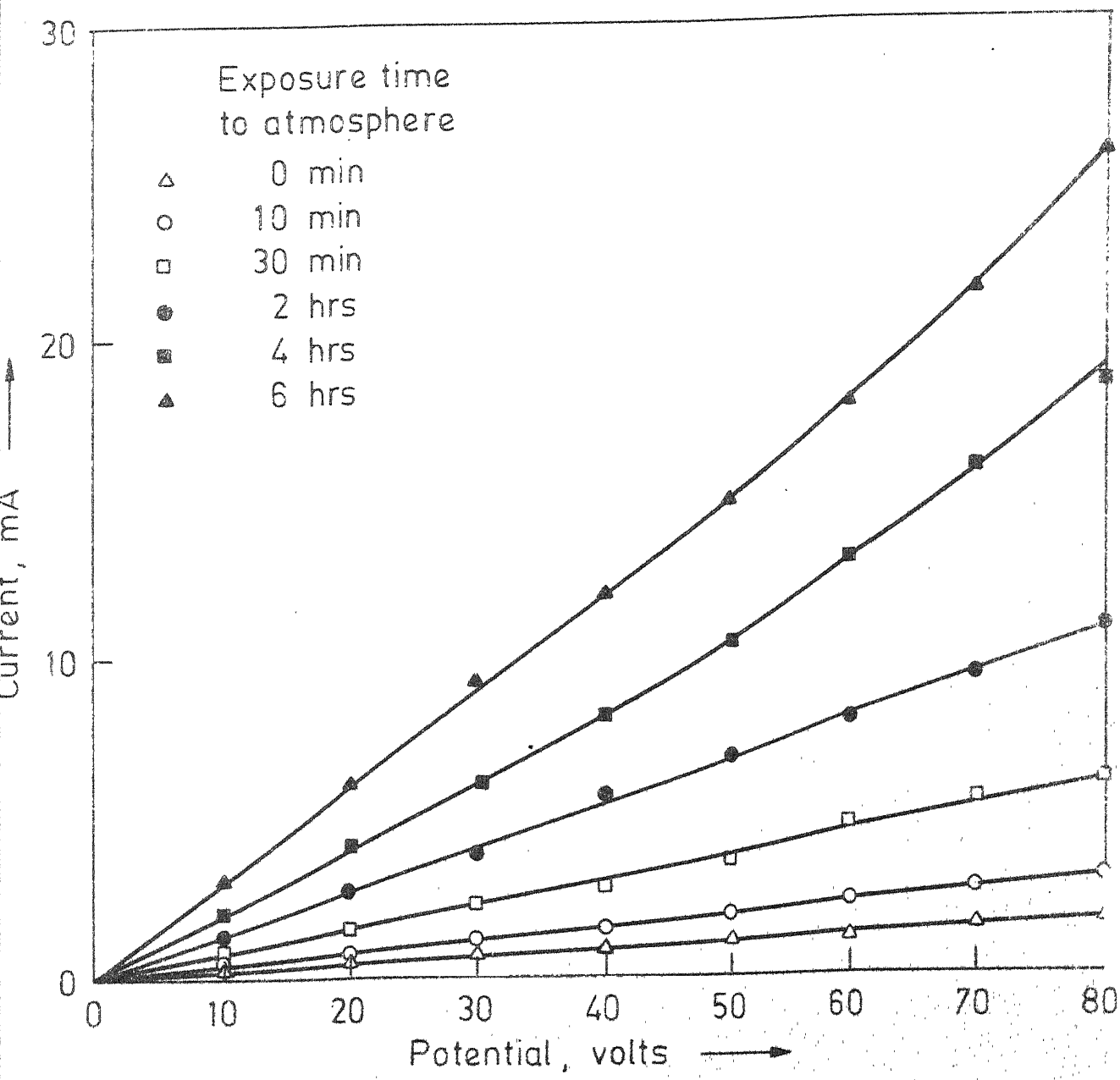

Fig. 3.13 - Potential - current curves for D.I. water.

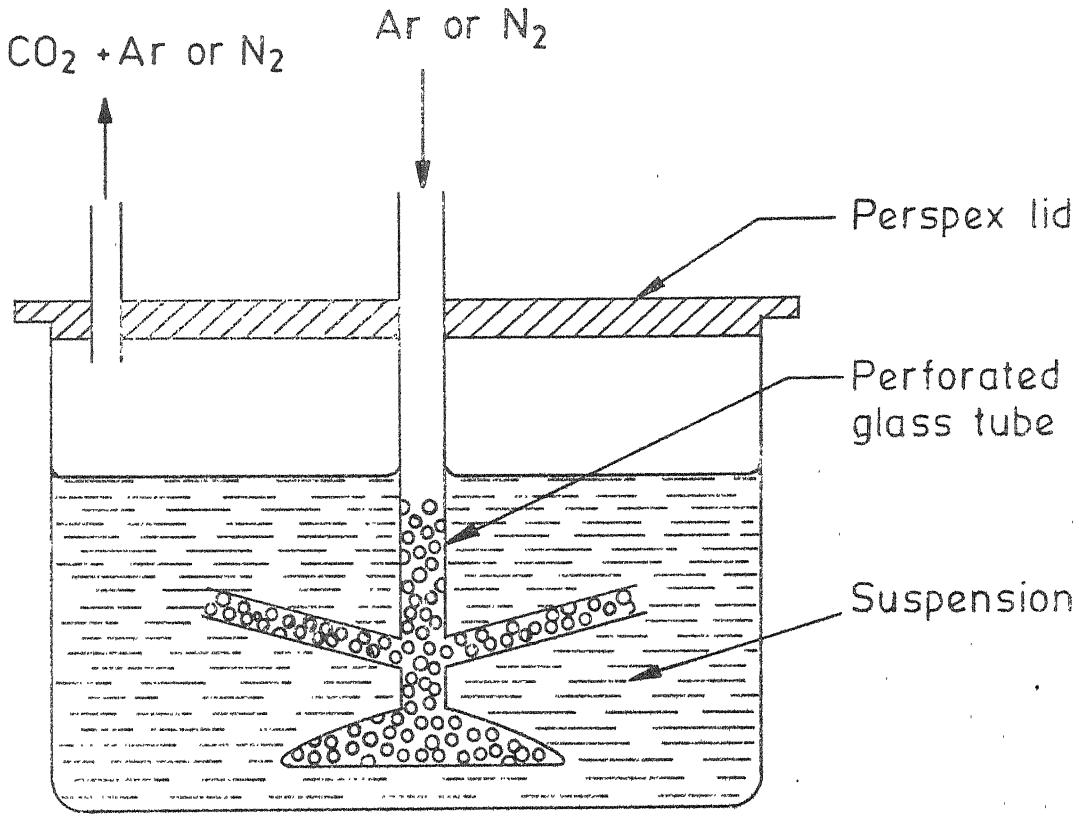

Fig.3.14- Arrangement to remove the dissolved CO_2 from suspension.

or flaked off the substrate. This action was jointly caused by the anode gas being evolved, a phenomena which increased with voltage and thus current, and the escape of water from the film on drying. Thus, the amount of water that would escape on drying from any given film increased with the thickness of that film, thereby creating numerous cracks and fissures in the plate.

After examining several films at various voltages and time a satisfactory plate was achieved using 30 volts for 1.5 min. and at 3.2 per cent PWC. These conditions were maintained throughout the plating experiments conducted on each powder.

In order to determine the optimum pH, a series of platings were conducted at various pH values in the range of 3.6 to 10.00. The results of these experiments are shown in Figure 3.15, where pH plotted vs film weight. As can be seen from Figure 3.15 a pH of 6.5 to 7.0 will result in a plate of maximum film weight. A similar plot for NiO is incorporated in the Figure 3.16.

Figure 3.16 presents the curve of film weight vs time used to determine the length of drying time necessary at room temperature to ensure that all the water in the film has escaped. As can be seen it is safe to assume that all the water has escaped after about 5 to 6 hrs of drying.

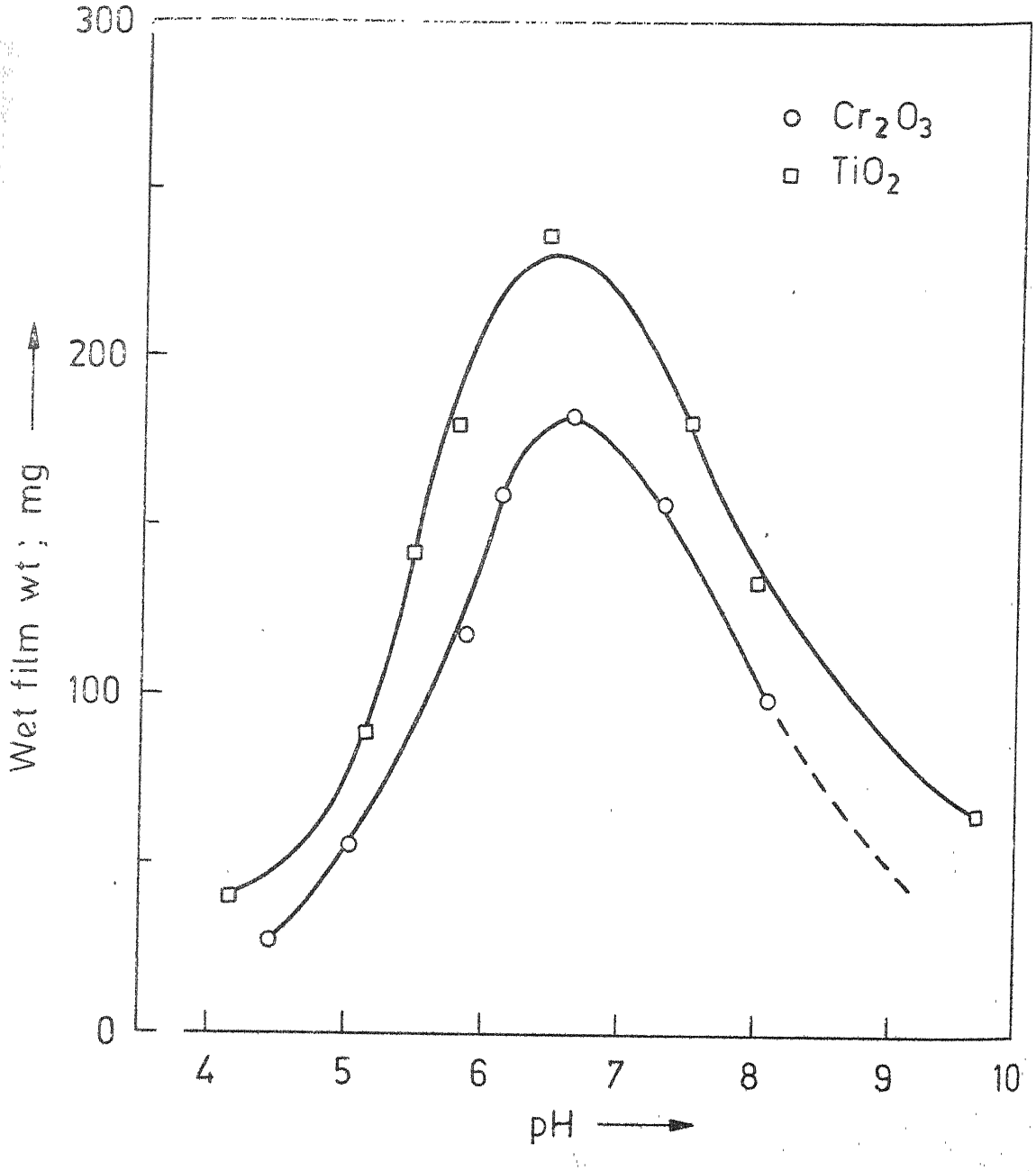

Fig. 3.15 - Graph of wet film weight vs pH for TiO_2 and Cr_2O_3.

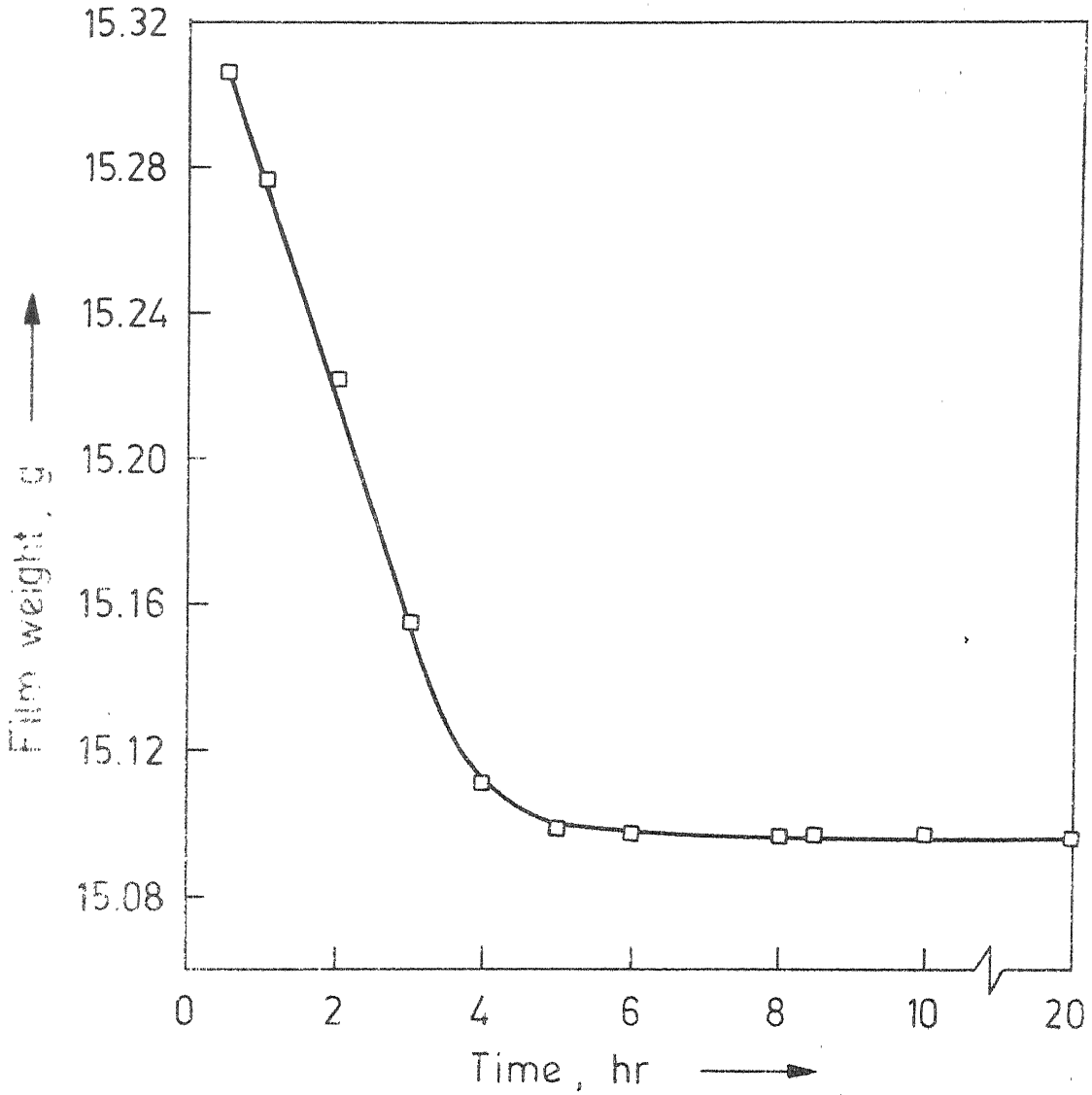

Fig 3.16 - Graph of film weight vs time for TiO_2 deposit at room temperature.

Deposition of Al_2O_3

The mobility and zetapotential profiles for alumina do not show the peaks to obtain a close pH range desired for deposition. Therefore, before arriving at optimum conditions for deposition of alumina on graphite substrates, the kinetics studies were undertaken.

Experimental

The same experimental procedure was followed for alumina deposition as that described earlier for TiO_2. The anodes were rectangular graphite plates of 5.50 cm x 1.35 cm and about 1 mm thick. They were polished upto 3/0 paper and further with linen cloth to give very shining and smooth surface. The electrodes were boiled in distilled water, dried in an oven and then cleaned with acetone.

Fresh suspension was used for each experiment.

Kinetics of Al_2O_3 Deposition

Effect of Deposition time and Current

Figure 3.17 shows that the current gradually decreases with time. Initially the current remains almost same. As the thickness of the deposit increases, it will offer greater resistance to current flow. The conduction after long periods is possibly through the electric double layer present around each particle.

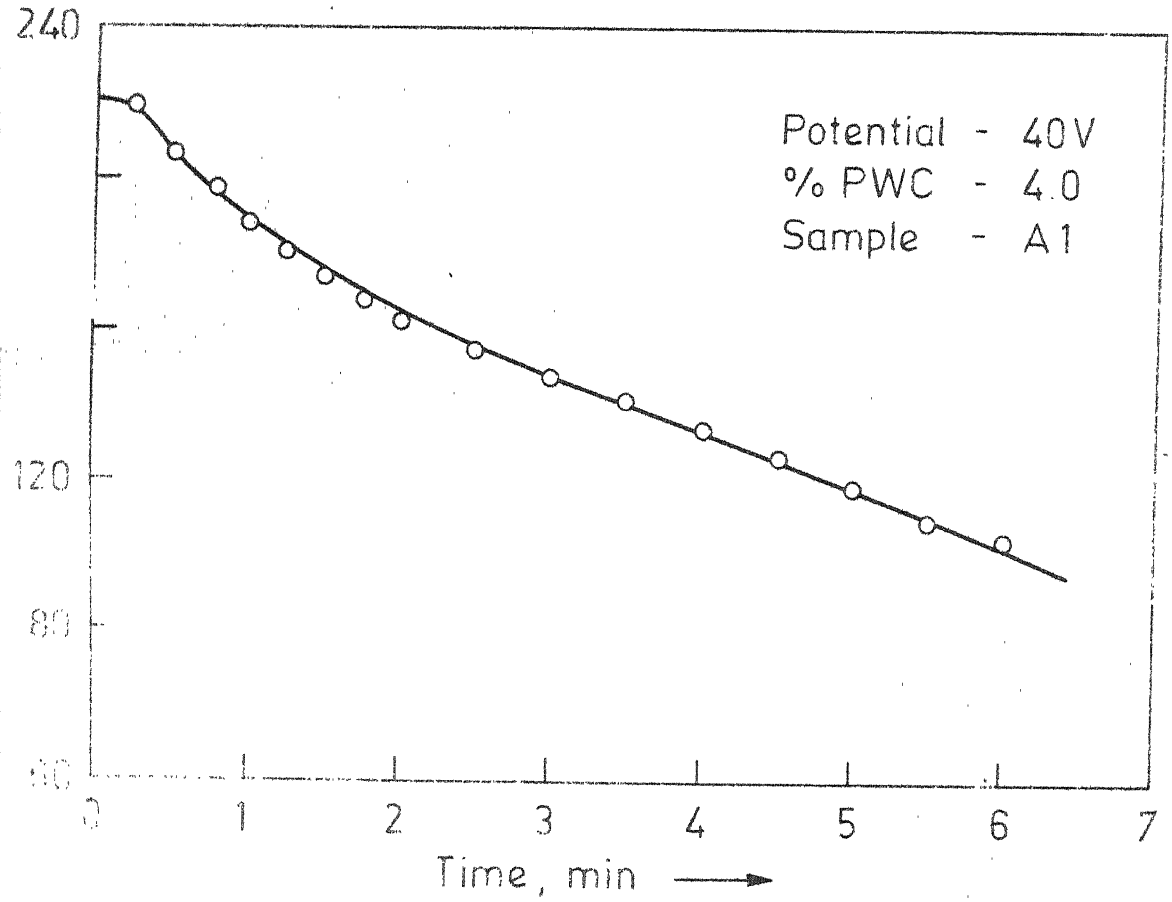

3.17 Variation in current during electrophoretic deposition for Al_2O_3

Effect of pH:

Figure 3.18 shows the variation of density, yield and thickness with pH of suspension of 3.2 per cent PWC. The other variables for example time 90 sec., voltage 30 v were kept constant. From the figure it is seen that thickness, yield and density decreases after the pH value of 8.3.

Effect of Solid Concentration

Figure 3.19 shows that increasing amount of solid concentration of the suspension improves thickness and yield. The density values, however, come down after the peak value of 3.2 per cent PWC. The reason for the decrease in the density values at higher concentration is, rise in the conductivity resulting in higher currents leading to the gas evolution at the anode. This leaves the deposit porous and accounts for lower density values of the deposits.

Effect of Time

For a given suspension concentration i.e. at 3.2 per cent PWC, pH range 7.8 to 8.2, and 30V, the thickness and yield increases with time. From the Figure 3.20 the density values after 90 seconds lower down.

Effect of Voltage

The effect of voltage was qualitatively studied. Higher voltages correspond to the deposits having cracks and fissures.

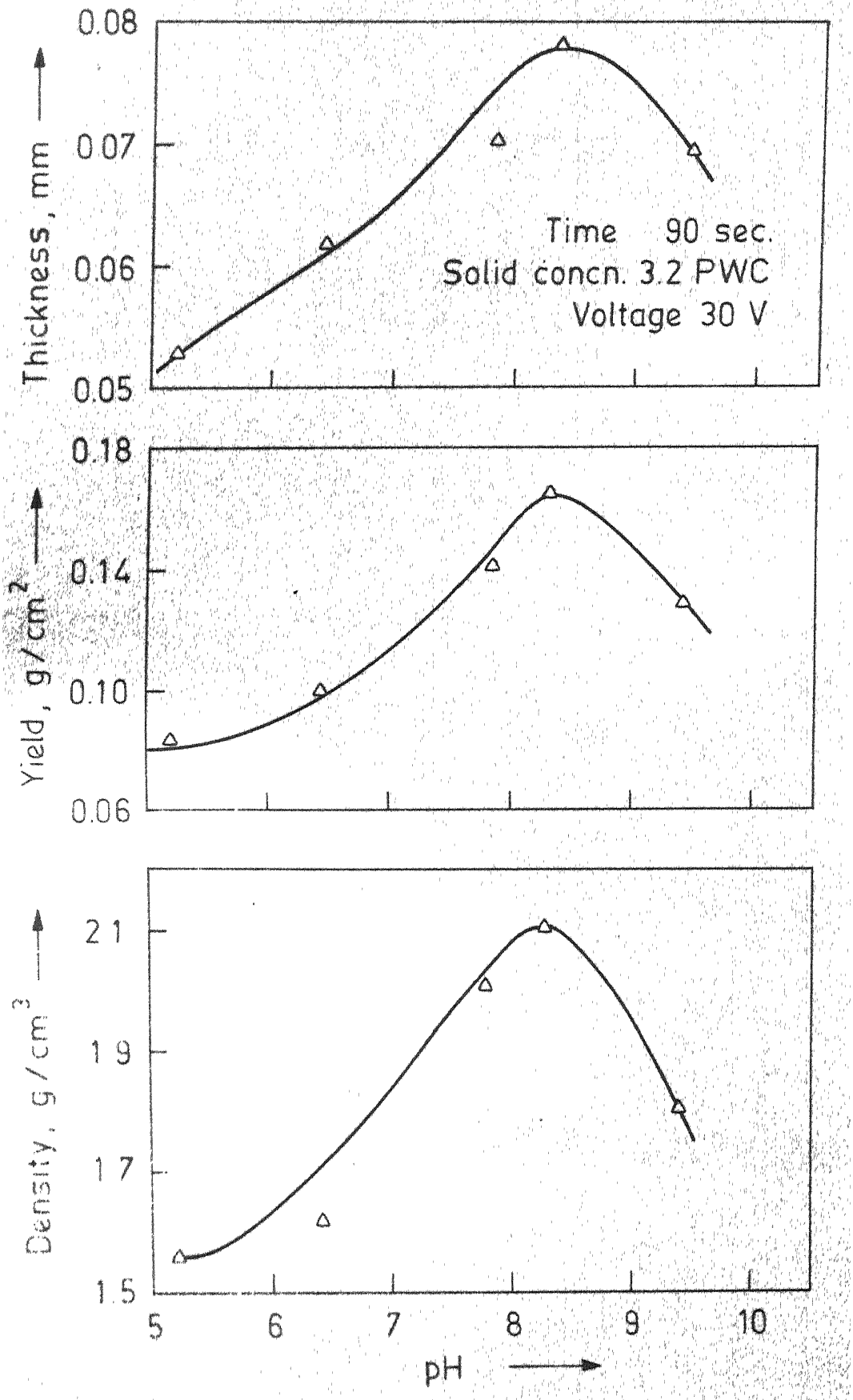

Fig 3.18 - Variation of thickness, yield and density of Al_2O_3 (A1) deposit with pH of the suspension.

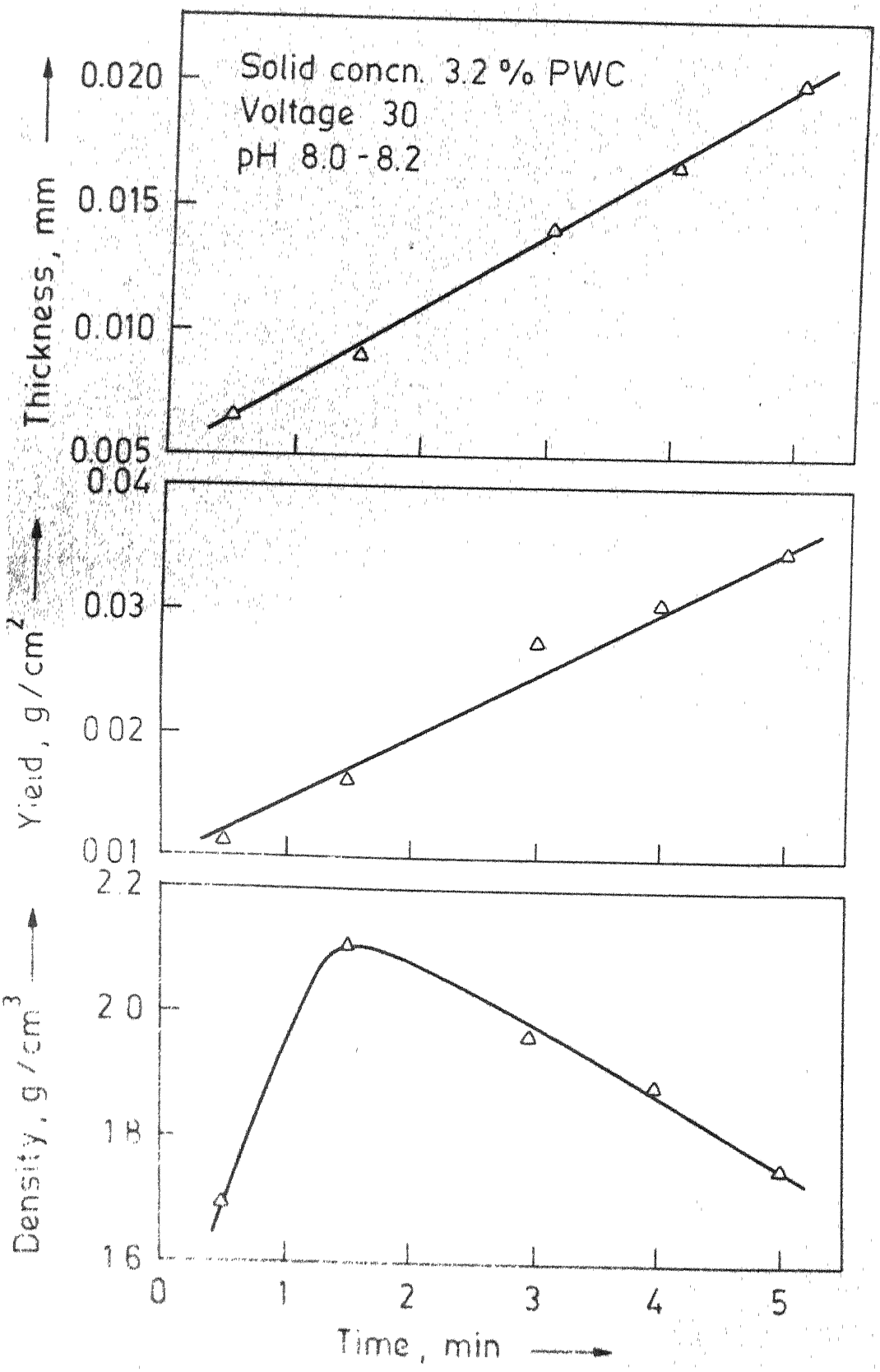

Fig 3.20 - Variation of thickness, yield and density of Al_2O_3 (A1) deposit with time.

Coulombic Yield for Al_2O_3

The weight of film deposited may be calculated as a function of current. The coulombic yield, the mass of oxide deposited per coulomb of electricity is of prime interest.

To keep the solid to binder ratio constant, for an increase in PWC, there must be an increase in the binder. The result of this increase in dispersant is an increase in the conductivity of the suspension thereby increasing the flow of current at a constant voltage. The number of coulombs thus, can be calculated with the knowledge of current flow and the time of deposit. Thus, knowing the weight of the oxide deposited, the coulombic yield may then be determined.

Table 3.3 and Figure 3.21 represent this data. From Figure 3.21 it can be seen that with an increase in the current the coulombic yield decreases for alumina untreated samples A1 and A2. For the treated sample, the yield increases with current, reaches maximum to 6.2 mg/coulomb at about 120 mA and then decreases with current.

During deposition there must be OH^- ions travelling with the particle to the anode. These ions must have an effect on the oxide particles. Thus, the particles are carried alongwith the OH^- ions to some extent. Since an increase in the PWC of the suspension necessitates an increase in dispersant, there must also be an increase in the organic base added to maintain a constant pH level. Thus, there is an

TABLE 3.3

Determination of Coulombic yield for each Al_2O_3 Sample

Sample	PWC %	Current (mA)	Coulombs (amp.xtime)	mg. deposited in 90 seconds	Coulombic yield mg/coulomb
A1	3.2	75	6750×10^{-3}	86.2	12.76
	4.0	114	10260	103.0	10.04
	4.8	216	19440	140.2	7.21
A2	3.2	80	7200	82.4	11.45
	4.0	115	10350	105.6	9.71
	4.8	220	19800	135.8	6.86
A2S	3.2	86	7440	45.4	5.87
	4.0	121	10890	68.8	6.31
	4.8	236	21240	105.0	6.19

All the runs performed under an applied voltage of 30 volts pH range 7.8 to 8.2 at room temperature for a period of 90 seconds.

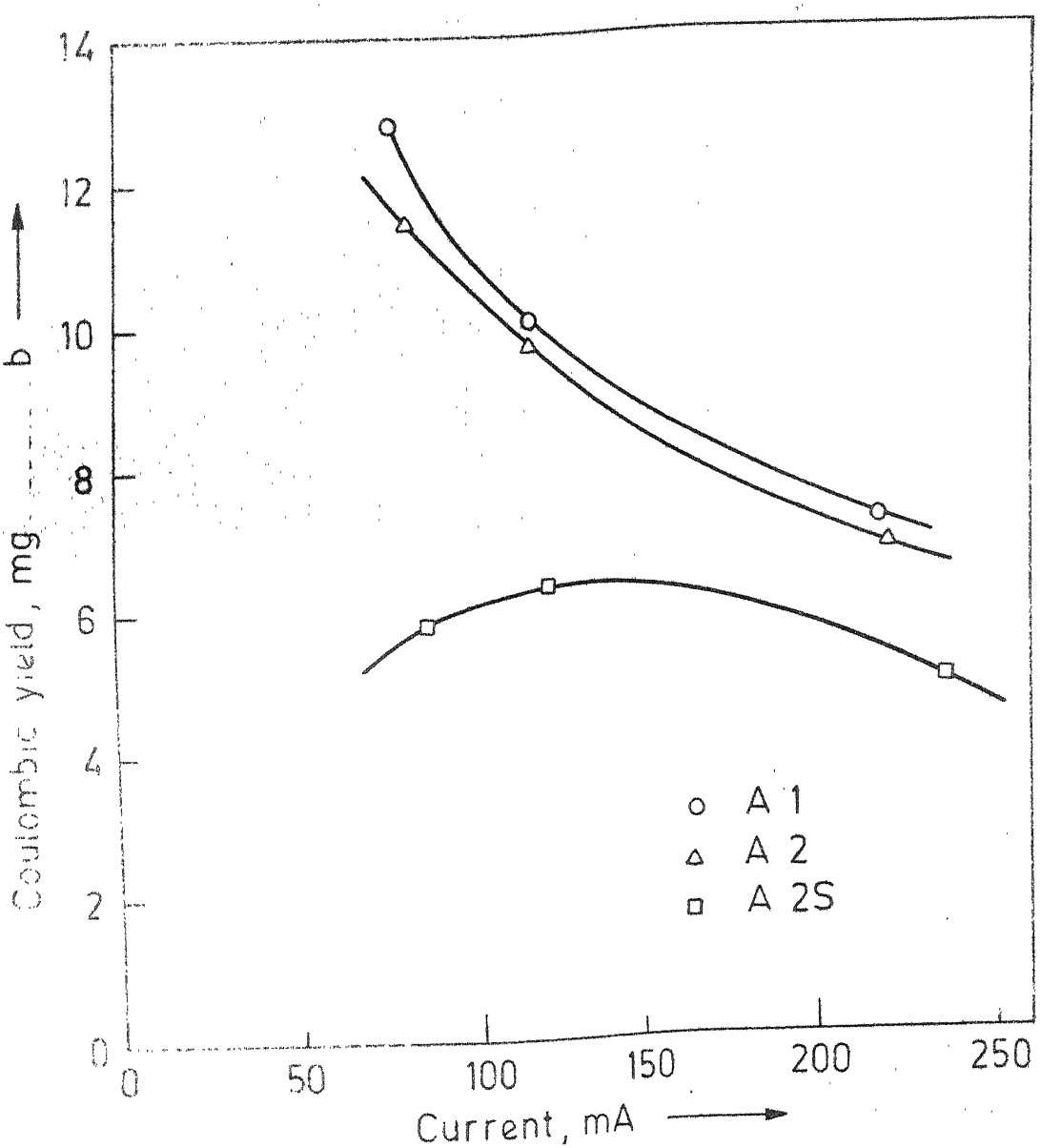

Fig. 3.21 Graph of coulombic yield vs current for Al_2O_3 samples.

increase in the OH^- ion concentration in the suspension with an increase in PWC. This accounts for an increase in coulombic yield, with an increase in current. The reverse behaviour exhibited by the untreated samples can be attributed to the fact that this oxide is less suceptible to foreign ions in the suspension.

Effect of Zetapotential on the Water Content of the Film

When oxide particles are suspended in polar medium, they form hydrogen bonds with OH^- ions in the medium. The extent of the formation of hydrogen bonds with the particles, depends on the electronegativity and thus, the number of sites available. During the migration of particles under an applied electric field, particles carry OH^- ions with them. Therefore, water in large quantity is present in the deposit. Thus, the interface potential (zetapotential) can be correlated with the water content in the deposit. Table 3.4 shows calculations for per cent water present in each Al_2O_3 sample.

Tables 3.5 and 3.6 present each powder together with the water content of the resulting films and zetapotential values read from the Figures 3.8 and 3.9 at proper deposition pH. As can be seen, for each PWC, the per cent water increases with the zetapotential, indicating that the particles or micelles must attract the polar water molecules and incorporate them into the original film.

TABLE 3.4

Calculation of Percent Water present in each Al_2O_3 Sample

Sample	PWC %	Wet film weight, gm	Weight of H_2O gm	% Water
A1	3.2	0.146	0.091	64.3
	4.0	0.167	0.105	62.8
	4.8	0.224	0.135	60.1
A2	3.2	0.139	0.095	68.5
	4.0	0.165	0.107	64.5
	4.8	0.220	0.136	61.8
A2S	3.2	0.077	0.055	71.2
	4.0	0.115	0.078	67.4
	4.8	0.214	0.134	62.6

All the runs were performed under an applied voltage of 30 volts in the pH range 7.8 to 8.2 at room temperature for a period of 90 seconds.

TABLE 3.5

Zetapotential and Percent Water in the Deposit

PWC %	pH	Zetapotential[φ] -mv	Percent Water %
3.2	7.95	53.0	64.3
	8.10	69.5	68.5
	8.15	146.5	71.2
4.0	7.8	52.6	62.8
	8.1	69.5	64.5
	7.9	143.2	67.4
4.8	8.0	53.2	60.1
	7.8	68.2	61.8
	8.0	145.0	62.6

φ Corresponding Zetapotential values are read from Fig. 3.8 and 3.9.

TABLE 3.6

Zetapotential and Weight of Water in Deposits

PWC %	pH	Zetapotential$^{\varphi}$ -mv	Weight of Water mg
3.2	7.95	53.0	91
	8.10	69.5	95
	8.15	146.5	55
4.0	7.8	52.6	105
	8.1	69.5	107
	7.9	143.2	78
4.8	8.0	53.2	135
	7.8	68.2	136
	8.0	145.0	134

φ Corresponding Zetapotential values are read from Fig. 3.8 and 3.9.

It should also be noted that the per cent water content of the film increases with a decrease in PWC but contains more water by weight than the one resulting from a low PWC suspension. (Table 3.4). Thus, the two representations in the Tables 3.5 and 3.6 show opposite trends.

Effect of Zetapotential on the Weight of Al_2O_3 Deposited:

From Table 3.7 an increase in zeta potential results in a decrease in the weight of Al_2O_3 deposited. Further, it is seen that an increase in PWC results in an increase in the weight of Al_2O_3 deposited, but a decrease in per cent water present in the film (Table 3.4) at constant zetapotential. This is evident from the fact that films at the lowest PWC value (3.2 per cent PWC) contained the highest weight per cent of water. It should be noted, again that these films actually contained the lowest amount of water by weight (Table 3.4), but because of the small weight of Al_2O_3 deposited on these plates, the per cent water becomes high.

Thus, suspensions containing particles of high zeta-potential produce thinner films than those containing particles of a lower zeta potential level, at constant PWC. However, an increase in PWC results in a definite increase in the weight of pigment deposited.

TABLE 3.7

Zetapotential and Weight of Al_2O_3 Deposited

PWC %	pH	Zetapotential$^{\varphi}$ -mv	Weight of Al_2O_3 mg
3.2	7.95	53.0	86.2
	8.10	69.5	82.4
	8.15	146.5	45.4
4.0	7.8	56.2	103.0
	8.1	69.5	105.6
	7.9	143.2	68.8
4.8	8.0	53.2	140.2
	7.8	68.2	135.8
	8.0	145.0	105.0

φ Corresponding Zetapotential values are read from Fig.3.8 and 3.9.

Relationship Between the Weight of Al_2O_3 Deposited and the Number of Coulombs Passed:

The relationship between the number of coulombs passed and the weight of Al_2O_3 deposited is given in Table 3.3 and Figure 3.22. From Figure 3.22 it is seen that untreated samples deposit in larger weight than the treated one (activated) at any constant level of coulombic flow. Furthermore, by referring to Figure 3.22, it is seen that untreated alumina sample No.A1 and A2 follows a linear relationship whereas, the treated alumina sample No.A2S in no way behaves in this manner. This disagreement by sample No.A-2S might be expected because of the surface treatment effect on the deposition of the particle.

Quality of the Deposits

Colour

All the deposits, immediately after the deposition and subsequent drying were white. The TiO_2, deposited on iron electrodes, after drying, exhibited yellow to brown stains at the upper part. This colouring is thought to be the result of the formation of iron hydroxide or other complexes of Iron and their diffusion into the deposits. The activated sample of alumina deposited on graphite substrate showed an yellow tinge throughout the surface.

Visual Study

The deposits obtained from PWC of 3.2 per cent for

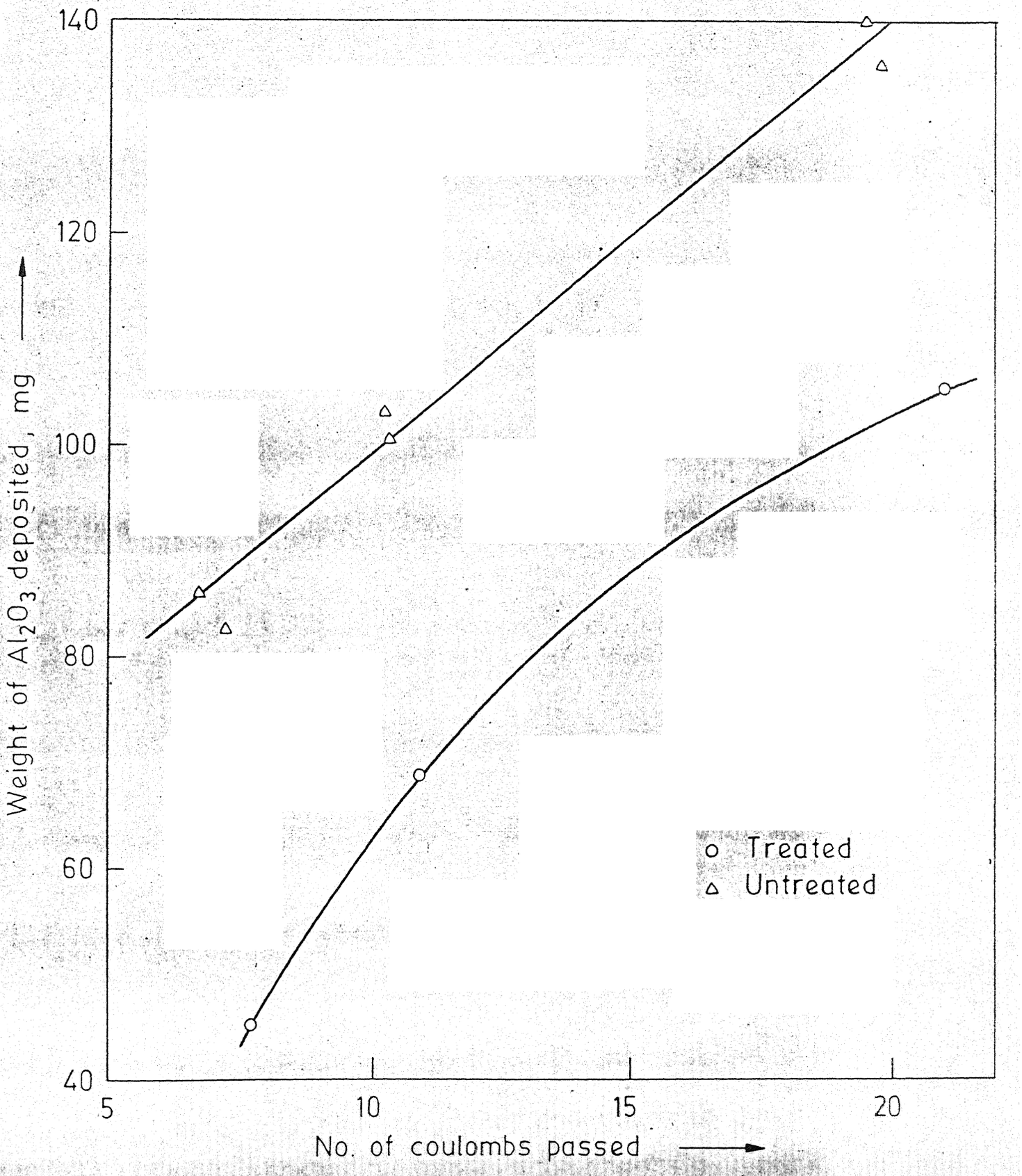

Fig. 3.22 Graph of weight deposited vs number of coulombs passed for Al_2O_3.

90 seconds x 30 volts were smooth and uniform with no cracks and porosity. Figure 3.23 is the photograph of the dried alumina deposits of sample A1 from PWC 3.2 per cent. This sample was deposited for 90 seconds at 30 volts. However, observing through the magnifying glass revealed some porosity and microcracks at the edges of the sample. This may be the result of non-uniform current density at the edges where there is a sharp change in the geometry.

The photograph (Figure 3.24) is of the sample A1, deposited at 30 V at PWC of 3.2 per cent for 180 seconds. The sample revealed many continuous cracks with the formation of little blow holes. Long deposition times yielded thick deposits which on drying cracked due to the escape of water.

The photograph 3.25 is of sample A2 deposited at 60 volts and PWC of 3.2 per cent PWC for 90 seconds. The sample before and after drying revealed blow holes and porosity. The high potentials for electrophoretic deposition from aqueous suspension causes the gas evolution and the anode and hence this defect.

The photograph (Figure 3.26) is of the sample A1, at PWC of 4.8 per cent for 90 seconds at 30 volts. The surface of the sample after drying appears to be that of moon. In this case, the alumina appears to have been deposited as agglomerates. High solid concentration of the suspension does not enable the particles to be in suspension individually but as agglomerates.

Summary

The effect of solid concentration, pH, voltage and time of deposition on the quality of film has been presented and discussed. Generally, the result of increasing the PWC is an increase in film cracking or peeling due to the escape of both the anodic gas and trapped water on drying.

The weight of oxide deposited was found to decrease with the number of coulombs passed. It is also noted that an increase in zetapotential resulted in decrease in the weight deposit.

The water content in the film increased with an increase in bath concentration.

In general, it is difficult to isolate each parameter in order to determine its contribution to the resulting film. However, it appears that PWC and pH are important, as these determines the thickness and water content of the film.

CHAPTER 4

APPLICATIONS

The science of electrophoretic deposition as developed in earlier chapter has been used to tackle some application oriented problems. The process of electrophoretic deposition has been developed to produce oxidation resistant coating on graphite substrate. Also, the coating of $NiO-Cr_2O_3$ on mild steel substrate has been undertaken in order to obtain stainless steel composite after chemical reduction. The experimental arrangement and results of this investigation are presented in this chapter.

4.1 Preparation of Nickel-Chromium-Iron Composites

4.1.1 Introduction

Alloy production, by plating of metal surface by another metal, has made significant strides in recent years, chiefly to bring out uniform platings. As an example, chromium coating on steel is now-a-days achieved by sprinkling of powdered chromium metal or pastes on the substrate followed by annealing treatment. The uniformity of the plating depends on the ability to create a uniform powder coating.

Even though, elements like Cr and Ni could be deposited by high frequency induction heating in vacuum [32], the

technique cannot be universally acceptable as it is not economical, from the stand point of high frequency current and expensive equipment. Also, powdered metals or pastes must be applied prior to the induction heating procedure.

The use of electrophoresis in the plating of metal substrates has been examined by Sturgeon and Armstrong [29], the plating bath consisting a methylated solution containing 10 per cent $H_2O$and 1 millimole/l $Al(NO_3)_3$. The steel strip which was being plated was coated with 5 micron carbonyl nickel powder from this suspension, which amounted to a thickness of 1 to 3.4 mils after rolling with 90 tons/in^2 pressure.

Caley [10] in 1972 has used this technique of electrophoresis to produce a coherent and uniform composit of Fe-Cr-Ni on iron substrate. The electrophoretic bath was an aqueous suspension of a mixture Cr_2O_3 and NiO with polyacrylic acid and triethylamine.

Preparation of stainless steel composites by using the technique of electrophoretic deposition was the aim of the present investigation. The information available for TiO_2 system has been the basis of investigation in the development of bath from which NiO and Cr_2O_3 could be deposited. The sintering of NiO + Cr_2O_3 deposit under the hydrogen atmosphere may lead to the formation of stainless steel coating.

4.12 Experimental

The procedure used in determining the optimum plating conditions for TiO_2 was followed in order to realize the optimum plating conditions for NiO and Cr_2O_3. Using the information as the pH range (Figures 3.6 and 3.7) and per cent PWC which yielded the best TiO_2 platings simplified the process. A PWC 3.2 per cent in a pH range of 6.5 to 7 was found to produce the best films.

In order to plate NiO and Cr_2O_3 on an iron substrate, the Cr_2O_3 was plated on NiO surface as well as from a Cr_2O_3-NiO mixture, with no difference in the quality or thickness of deposit. However, plating from the NiO-Cr_2O_3 bath is desirable because of the advantages of plating from the mixed bath.

As there was a gradual rise in pH of the bath with plating, it was necessary to add polyacrylic acid to the bath after three-four platings. During plating in each case the current was reversed for 5 seconds midway through the plating. This was found to eliminate any points of concentrated film growth, and resulted in each deposit being uniform and smooth.

Reduction of NiO-Cr_2O_3 Deposits

The reduction of the deposited sample was carried out by flowing hydrogen over the samples. Argon was used to flush the system before and after the hydrogen flow to ensure

that there was no residual oxygen in the system. Ultrapure hydrogen was used, and temperature was 1300° C.

A horizontal silicon carbide furnace was used for the reduction. The experimental arrangement is shown in Figure 4.1. The hydrogen is continuously passed through a bubbler, and fused $CaCl_2$ and finally into the furnace tube made of recrystallized alumina. The reaction products were made to pass into a sulphuric acid bubbler before being passed into the atmosphere.

The furnace temperature was measured using a Platinum-Platinum 13 per cent Rhodium thermocouple. The temperature was controlled to an accuracy of $\pm$ 5°C.

The samples to be reduced were secured in position by means of a slot created with the zirconia boats. Titanium sponge was placed in the boats nearer to the sample as shown in the Figure 4.1. The purpose of this was to use the minimum possible hydrogen flow rate, as it regenerates the hydrogen from reaction products. The chemical reaction of the interest is as below

$$H_2O + T_i \text{ ——————— } TiO_2 + H_2 \qquad (4.1)$$

The reduction was carried out at 1300°C for 28 hours. The samples were furnace cooled, and then sectioned for microstructure and hardness measurements.

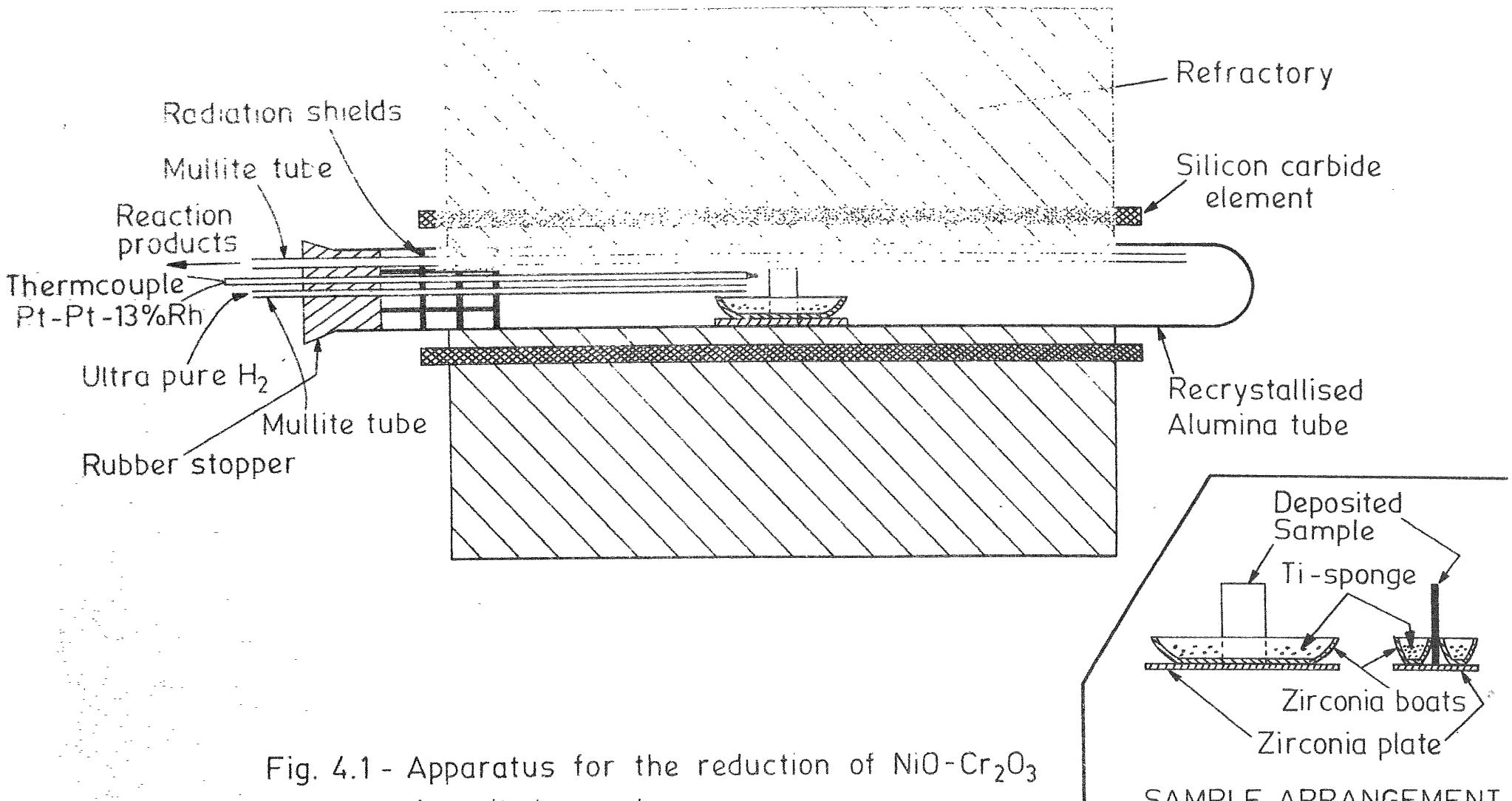

Fig. 4.1 - Apparatus for the reduction of $NiO-Cr_2O_3$ deposited samples.

4.1.3 Results and Discussions

Chemical Analysis of NiO and Cr_2O_3 in the Deposited Film from the Mixed Baths

The electrodes were plated from a mixture of NiO and Cr_2O_3 baths with varying ratios. Table 4.1 shows the chemical analysis of NiO and Cr_2O_3 contents in the coatings.

TABLE 4.1

CHEMICAL ANALYSIS OF NiO-Cr_2O_3 DEPOSITS

Sample No.	Cr_2O_3:NiO in the bath	Per cent Cr_2O_3 in the film	Per cent NiO in the film	Cr_2O_3: NiO in the film
4	1:1	51.82	48.18	1.05:1
8	1:1	54.22	45.78	1.18:1
15	2:1	66.21	33.79	1.98:1
18	3:1	71.45	28.55	2.58:1
49	3:1	71.38	28.62	2.70:1
50	3:2	60.38	39.62	3.00:2

Note: All the runs were made at 3.2 per cent PWC for 180 seconds, 30V, and pH 6.5 at room temperature.

From the data in the Table 4.1 it can be seen that the ratio of NiO and Cr_2O_3 in the film is almost same as that of the bath from which the plating was obtained. This can be further emphasised that mobility of Cr_2O_3 and NiO appear to be almost same and thus, would deposit in the same ratio.

Visual Study of the Reduced Samples:

The samples were partly reduced. At the edges it showed a metallic luster. A shining streak of 3 mm to 4 mm width was observed at the upper part of the deposit. After scrapping off the deposit, the inner surface was shinning. This may be the result of diffusion of hydrogen at high temperatures through the pore structure in the deposit thereby, reducing Fe-Cr_2O_3-NiO complexes to Fe-Cr-Ni composites.

Microstructure and Microhardness:

A transversed section from the reduced site of the plate was cut, mounted, polished and etched with 5 per cent Nital. The photograph of the microstructure is shown in Figure 4.2. It shows the case and core distinctly. The case is thought of Fe-Cr-Ni composite on the core of ferrite. The structure is annealed.

The microhardness of the core and the case is 182 DPH and 234 DPH respectively.

Note: The further work is in progress.

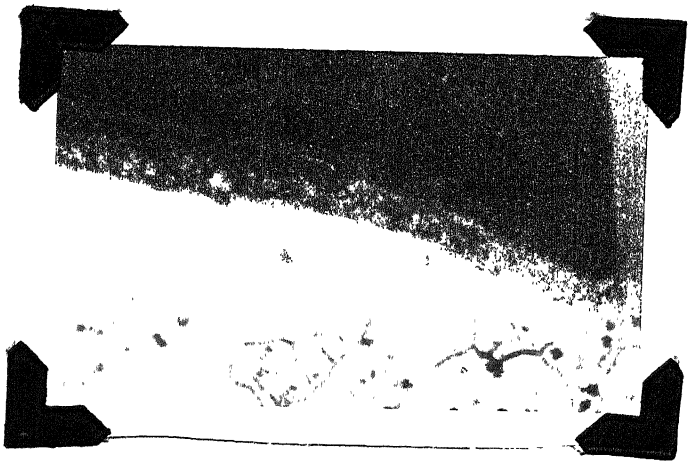

Fig.4.2 Microphotograph of reduced sample

Magnification X 400, Etched with 5% Nital.

4.2 Preparation of Oxidation Resistant Alumina Coatings on Graphite

4.2.1 Introduction

Metallurgical applications of electrophoretic deposition of ceramic compounds on metal and graphite surfaces has already been emphasised. Special protective surfaces may be produced by depositing ceramic compounds electrophoretically followed by sintering or post chemical reactions [11].

The deposition of alumina on graphite is of significance in the light of a variety of potential applications. A coherent sintered deposit would impart much valued oxidation resistance to the graphite surface. This will be of wide ranging applications in all cases where graphite is exposed to oxidizing atmosphere. The process may also be used in various alumina shapes particularly crucibles and flat plates of dense or porous materials. Some results in the aforesaid direction are presented here.

4.2.2 Experimental

4.2.2.1 Experimental Materials

Alumina : Polishing grade (imported) particle size ranged from 0.3 to 0.8 μ.

Graphite: Rods were obtained from Eveready cells (1.5 V). The grade of the material was same as described in Chapter 3.

Procedure

Graphite rods of length 2 cm were fired at 750°C under vacuum for 15 to 20 mnts to get rid of volatile matter and surface impurities. Then they were polished with Linnen cloth. These samples were boiled in distilled water for about 1 hour and dried in an oven. The specimens were sealed in envolope and kept in desiccator until used.

The same experimental procedure for deposition of alumina on graphite was followed as described earlier in Chapter 3. The circular cell geometry for deposition is shown in Fig. 4.3 The experimental details are given in the Table 4.2.

TABLE 4.2

Experimental Details for Coating of Al_2O_3 on Graphite rods

Al_2O_3 concentration in the suspension	2.4 %
Binder to oxide ratio	1:6
pH of the suspension	8.75-9.25
Voltage of deposition	30 V
Time	30 seconds.

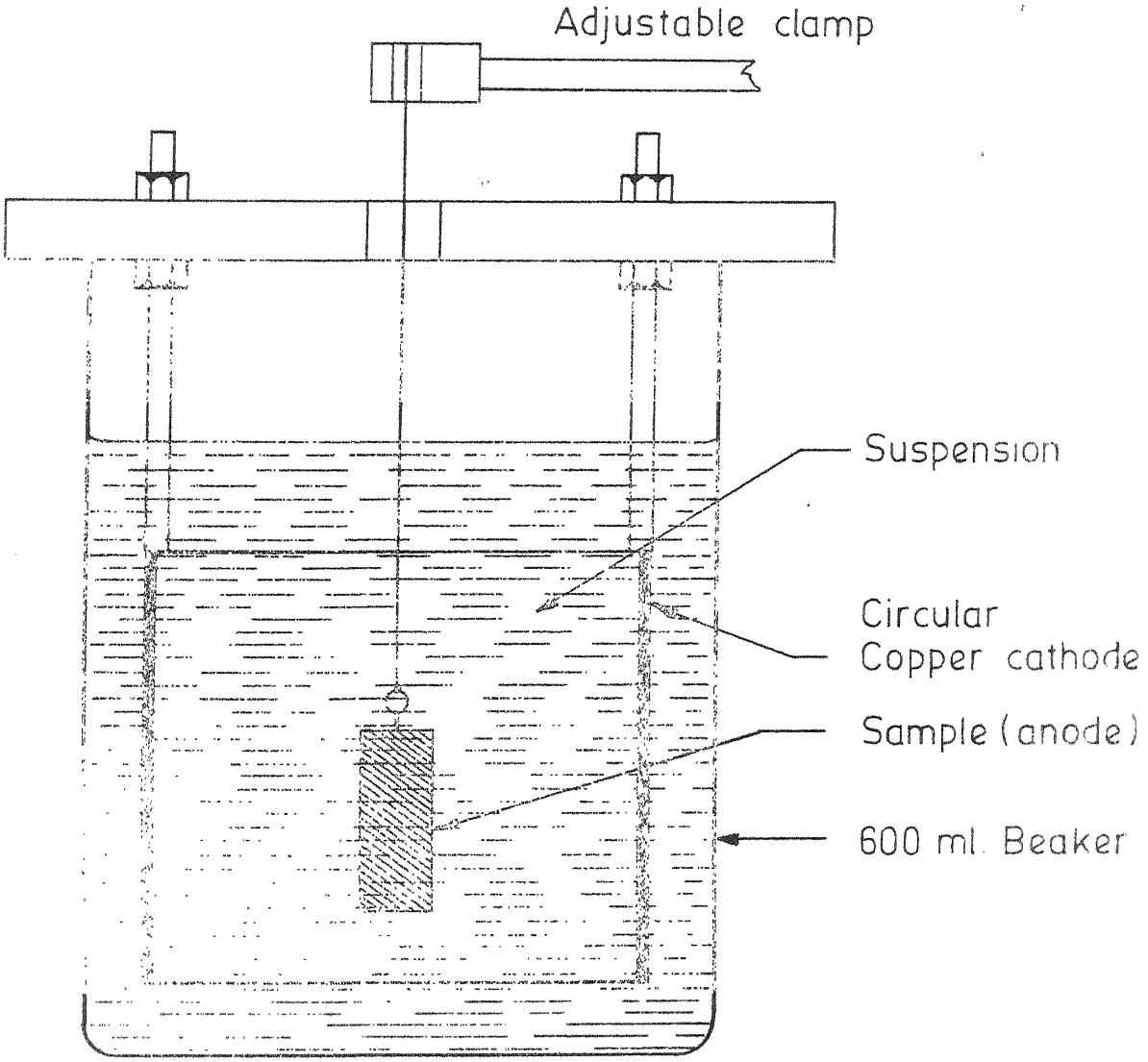

Fig. 4.3 - Electrophoretic cell arrangement.

Fig. 4.4 shows some alumina coated graphite rods before sintering. These rods were dipped in sodium-silicate (25 g/100 ml water), dried and then finally fired overnight at about 875°C. in an inert atmosphere of Argon. The oxidation characteristics of alumina coated graphite rods and those of uncoated ones taken from the same batch was carried out at different temperatures in stagnent air atmosphere. The oxidation assembly is shown in Fig. 4.5.

4.23 Results and Discussions

The oxidation characteristics of coated and uncoated graphite is shown in Fig. 4.6. From this figure it can be seen that the oxidation resistance of coated graphite with alumina has increased almost to 15 times than that of uncoated one. Fig. 4.7 shows the Arhenius plot for coated and uncoated samples. Both the profiles being parallel leads to the same reaction mechanism. The ash content of the graphite rods used in the present study was about 8 percent. It is felt that some of the impurities in the materials work as catalyst in the oxidation reaction by bringing down the activation energy. The activation energy in the present case was found to be 3.75 and 3.49 K cal/mole for coated and uncoated graphite respectively. Similar impurity effects have been reported by other workers [8].

Note: Further improvement work is in progress.

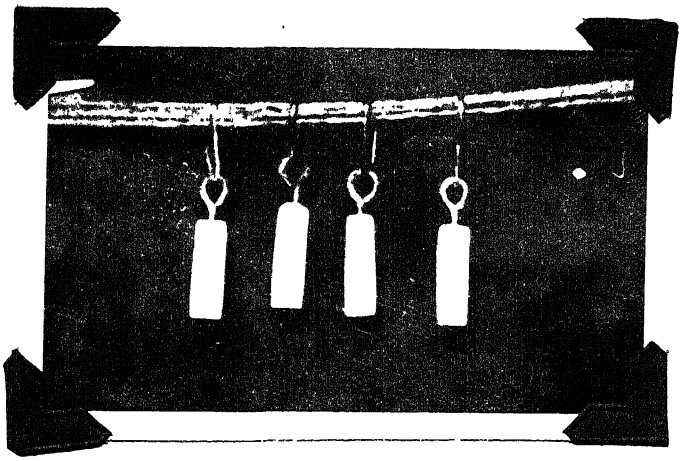

Fig.4.4 Alumina coated graphite rods after drying.

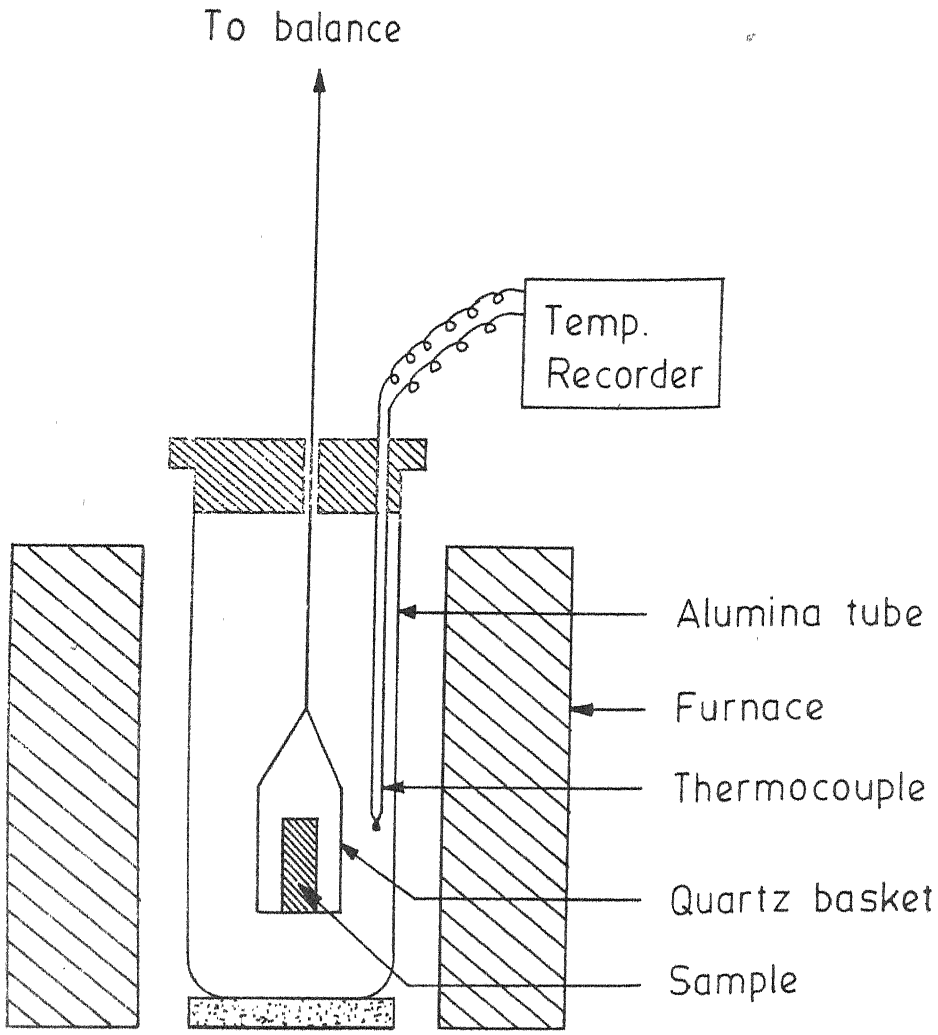

Fig 4.5 Apparatus for measuring the rate of oxidation of graphite and graphite coated alumina.

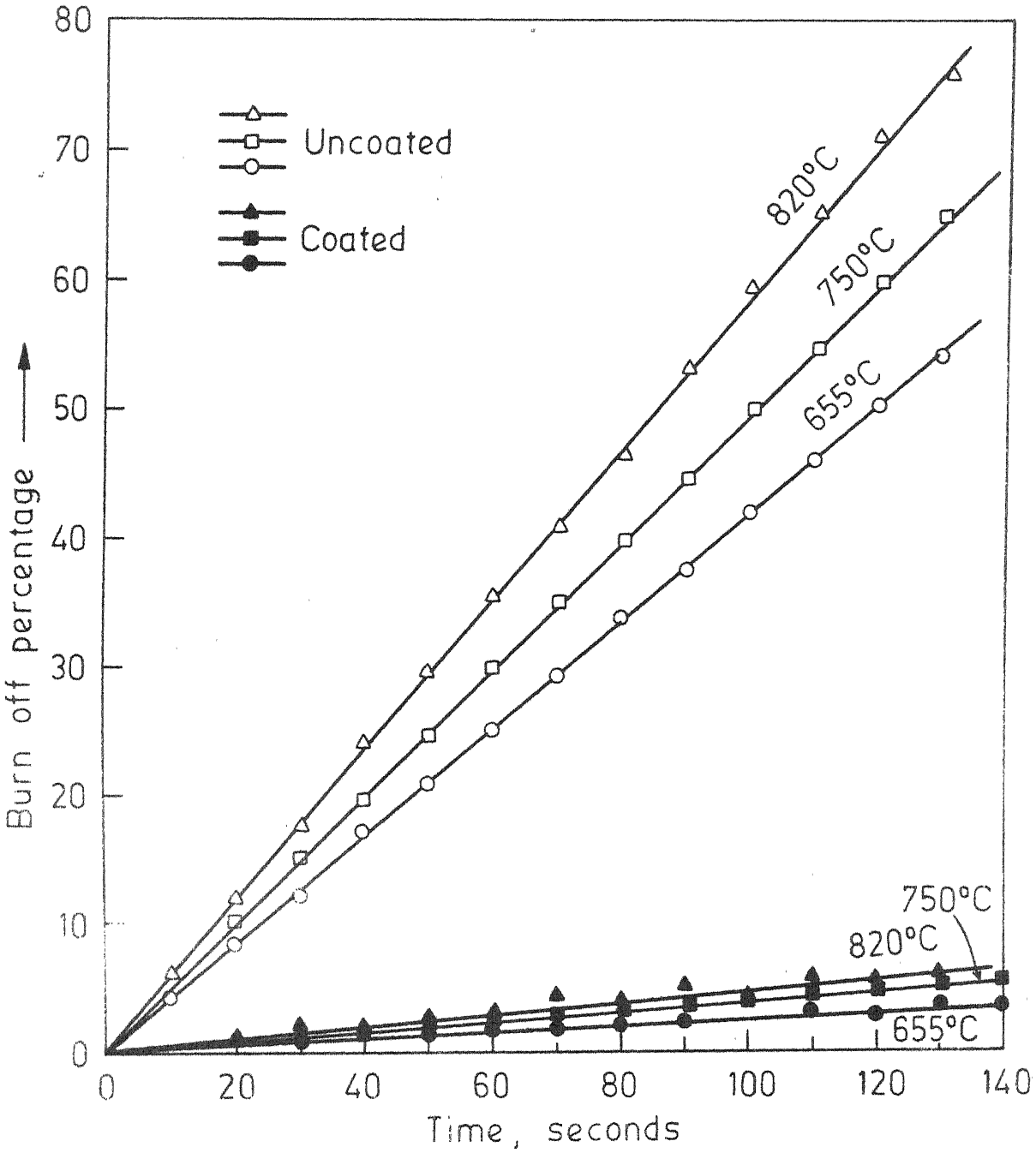

Fig. 4.6 - Oxidation characteristics of uncoated and coated graphite samples.

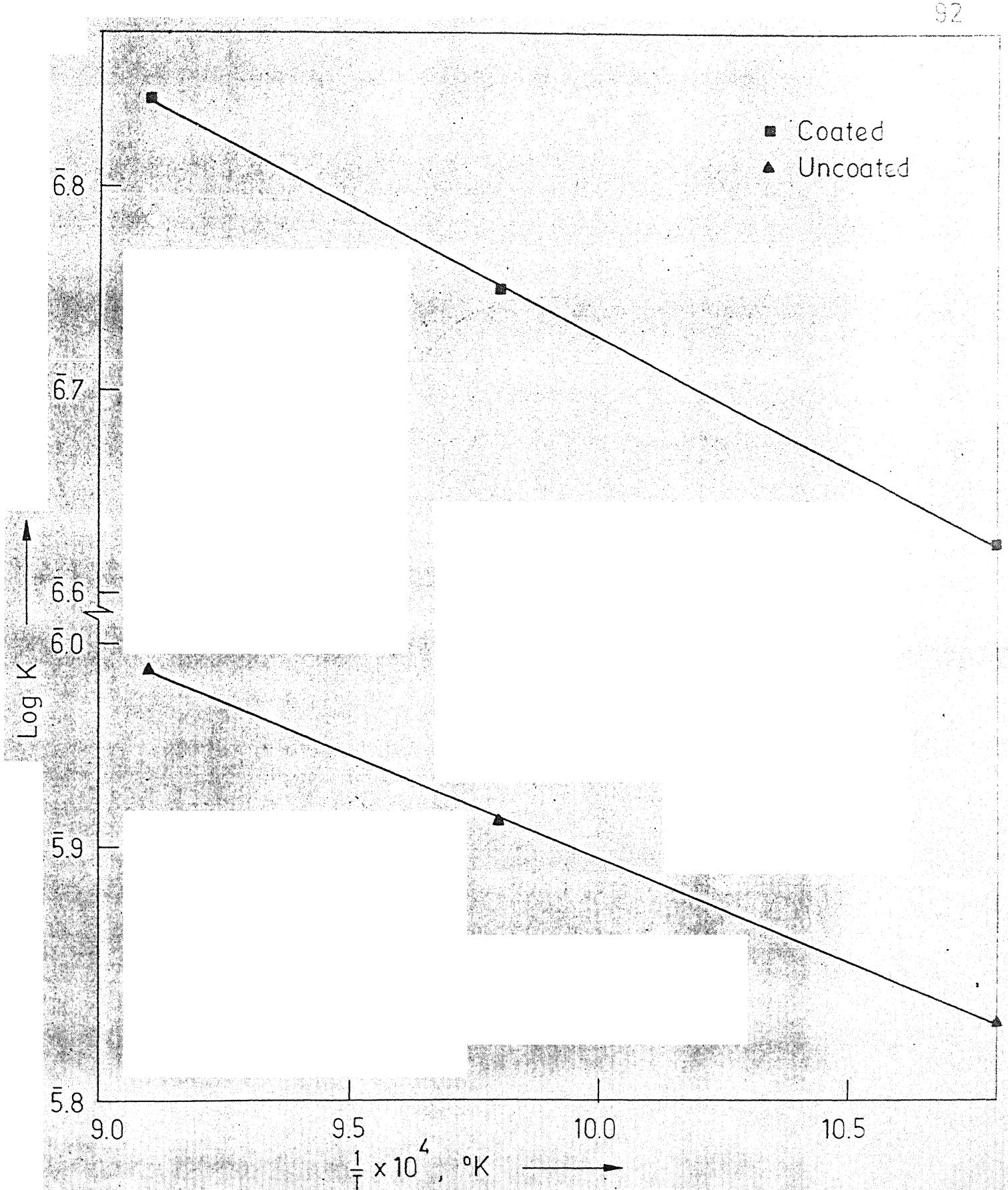

Fig. 4.7 - Arhenious plot for coated and uncoated graphite semple.

CONCLUSIONS

It is possible to deposit fine oxide particles TiO_2, NiO, Cr_2O_3 and Al_2O_3 on conducting surfaces from an aqueous suspension. The bath which exhibited optimum plating conditions consisted of 3.2 percent PWC, with a oxide to dispersant ratio 8:1 by weight. The dispersant used was polyacrylic acid, and the suspension brought to a pH of 6.5 to 7.0 by addition of the base tri-ethylamine. For Al_2O_3, the pH range was however, 7.8 to 8.2. It was found that plating times 90 to 120 seconds with a 5 second reversal of potential half way through the plating, produced best platings. All the platings were conducted under an applied constant potential of 30 V and a current of 75 to 100 milli-amps.

The quality of mixed NiO-Cr_2O_3 deposits remained same, whether deposited individually one over the other from separate baths or codeposited from a mixed bath. The Cr_2O_3:NiO ratio in the bath and in the coating was almost same

The use of this method of producing a nickel-chromium plating on mild steel has industrial applications, although, further work is needed to ascertain the post treatments.

Al_2O_3 powders have been deposited successfully on graphite substrates with the single aim to achieve oxidation resistant coatings. This method can equally be developed in forming alumina crucibles and tubes. The alumina coated graphite rods further coated with concentrated sodium silicate and finally sintered at about 900°C showed considerable oxidation resistance. At 850°C, Al_2O_3 coated graphite rods showed 15 times more oxidation resistant than uncoated ones. Our aim has been to get 100 folds increase or even more. This work is still in progress.

The fact that electrophoretic plating reaches all the parts of the piece being deposited regardless of the shape is a great advantage when plating corners and holes. Since the plating is carried out at room temperature, no additional equipment is required. The fact that only one bath is needed for co-deposition purposes is further saving in equipment costs, and the use of an aqueous rather than conventional organic media eliminates any fire hazards.

BIBLIOGRAPHY

1. Abramson, H.A., and L. Michaelis, J. Gen. Physiol. Vol. 12, (1929).

2. Adam, N.K., The Physics and Chemistry of Surfaces, Oxford University Press, (1941).

3. Alexander and Johnson, Colloid Science, Oxford University Press, (1949).

4. Andrews, J.M., Collins, A.H., Cornish, D.C., and Dracass, J., Proc. Brit. Ceram. Soc., Vol. 12, 211 (1969).

5. Anon, Painting by Electrophoresis Goes into Production, Metal working Production, March 6, (1963).

6. Benjamine, J., and Osborn, A.B., Trans. Faraday Soc., No. 36, 287 (1940).

7. Bier Millan., Electrophoresis - Theory, Methods and Applications, AP Inc., New York (1959).

8. Blackman, L.C.F., Modern Aspects of Graphite Technology, Academic Press, London (1970).

9. Bishwas, A.K., Surface Phenomena in Chemistry and Metallurgy, Department of Metallurgy, IIT Kanpur (1970).

10. Caley, W.F., Electrophoretic Deposition of Metallic Oxides and Production of a Composite Stainless Steel by High Temperature Reduction, Ph.D. Thesis, University of Toronto, (1972).

11. Choudhary, J.Y., Rai, K.N. and Ray, H.S., Electrophoretic Deposition of Ceramic Compounds from Aqueous Suspensions, to be published in Trans. I.I.M.

12. Das, R.K., Electrophoretic Deposition of TiO_2 from Aqueous Suspensions, M.Tech. Thesis, IIT Kanpur (1976).

13. Encyclopaedia Britannica, Vol. 8, Encyclopaedia Britannica, Ltd., Chicago, London, Toronto (1961).

14. Finn, S.R. and Mell, C.C., J. Oil Colour Chemists' Assoc., Vol. 47, 219,(1964).

15. Fisch, H.A., J. Electrochem. Soc., Vol. 119, No. 1, 57,(1972).

16. Glasstone, S., An Introduction to Electrochemistry, D. Van Nostrand Company, New York, (1975).

17. Glasstone, S., and Lewis, D., Elements of Physical Chemistry, D. Van. Nostrand Company Inc., New York, (1975).

18. Guthierrez, C.P., Mosley, J.R., and Wallace, T.C., J. Electrochem. Soc., Vol. 109, No. 10, 923,(1962).

19. Hasselberger, F., Allen, B., et.al., Biochem. and Biophysical Res. Commu. Vol. 57, 1054,(1974).

20. Holzinger, F., Paint Technology, Vol. 30, No. 8, 20, (1966).

21. Holzinger, F., Paint Technology, Vol. 30, No. 9, 26, (1966).

22. Kucharski, A.S., Deposition of Tungsten Carbide Surface Coatings, Toronto University (1972).

23. Powers, R.W., J. Electrochem. Soc., Vol. 122, No. 4, 490,(1975).

24. Polyacrylic Acids, Rohn and Hass, Philadelphia, (1972).

25. Raub, E., and Miller, K., Fundamentals of Metal Deposition, Elsevier Publishing Co., New York, (1967)

26. Senderoff, S., and Reid Jr., W.E., U.S. Patent 2, 2,843,541 (1958).

27. Shaw, D.J., Electrophoresis, Academic Press Inc., (1969).

28. Shyne, James, J., and Scheible, G. Howard, Modern Electroplating, T_S Section.

29. Sturgeon, George M., and Armstrong, Brian M., British Iron and Steel Assoc., No. 6, (1966).

30. Tawn, A.R.H., and Berry, J.R., J. Oil Colour Chem. Assoc. Vol. 48, No. 9, 790, (1965).

31. Werner, A.C., and Abbson, R.J., Preparation of Protective Coatings by Electrophoretic Methods, WADC Tech. Report 58-11 , (Feb. 1958).

32. Zemskov, G.V. and Gushchin, L.K., Chromizing of Steel by High Frequency Induction Heating in a Vacuum. Diffusion cladding of Metals, Edicated by G.V. Samsonov, Consultants Bureau, New York, (1970).

33. Zetameter Manual. Zetameter Inc., New York (1970).